

# **Looping-accelerated CO<sub>2</sub> Mineralization for Cost-competitive Cementitious Materials and Hydrogen**

## **Supplementary Information**

Kyle Shank<sup>1</sup>, Hefei Xu<sup>1</sup>, Yunming Xu<sup>2</sup>, Amirmohammad Arjomand Kermani<sup>1</sup>, Jiangzhou Qin<sup>1</sup>, Shang Zhai<sup>1,3</sup>

1 – Department of Mechanical and Aerospace Engineering, The Ohio State University, 201 West 19<sup>th</sup> Ave, Columbus, OH 43210, USA

2 – Department of Chemical and Biomolecular Engineering, The Ohio State University, 151 W. Woodruff Avenue, Columbus, OH 43210, USA

3 – School of Earth Sciences, The Ohio State University, 125 South Oval Mall, Columbus, OH 43210, USA

# Table of Contents

<b>Supplementary Figures</b> .....	<b>2-21</b>
<b>Supplementary Tables</b> .....	<b>22-32</b>
<b>Hydrogen Production</b> .....	<b>33</b>
<b>Technoeconomic Analysis Methods</b> .....	<b>33-44</b>
<b>References</b> .....	<b>45-47</b>

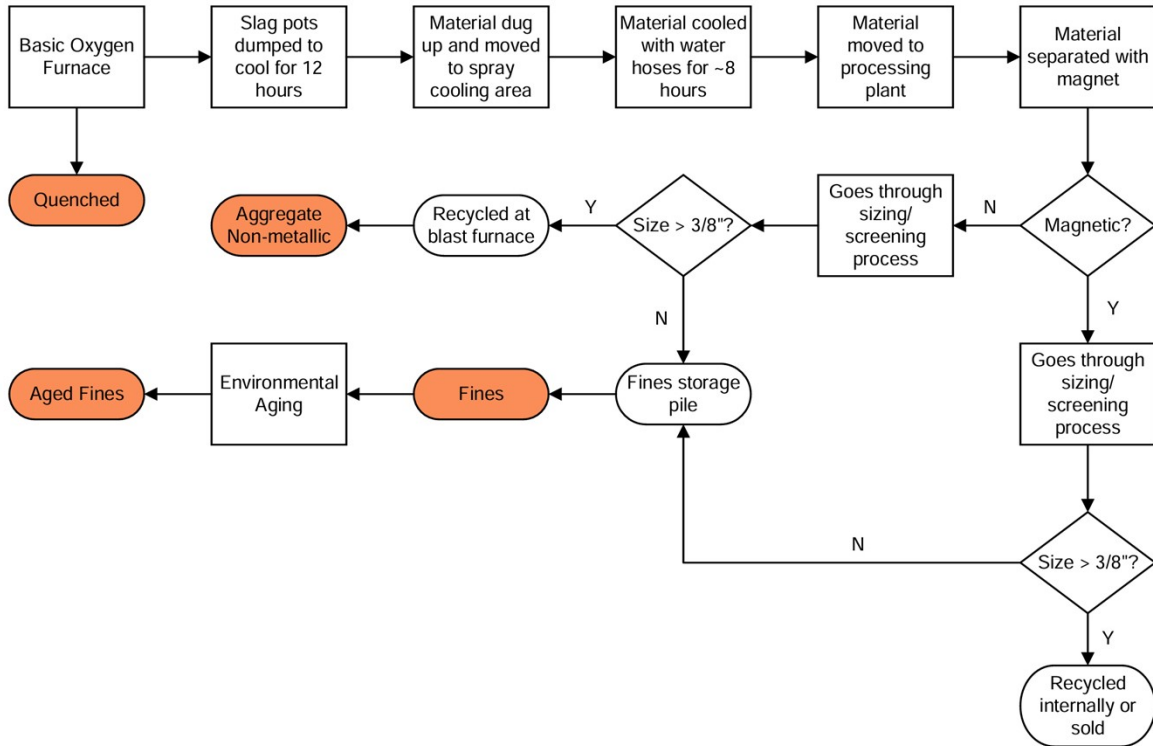


**Fig. S1** Cleveland-Cliffs – Cleveland Works BOF slag processing flow chart.

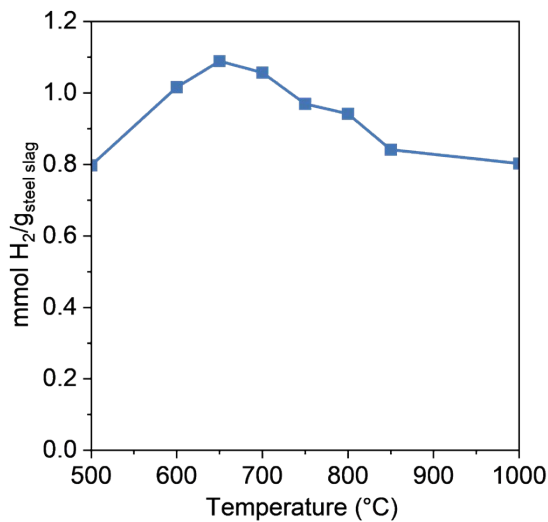


**Fig. S2** Dependence of hydrogen production on temperature for aggregate non-metallic slag.

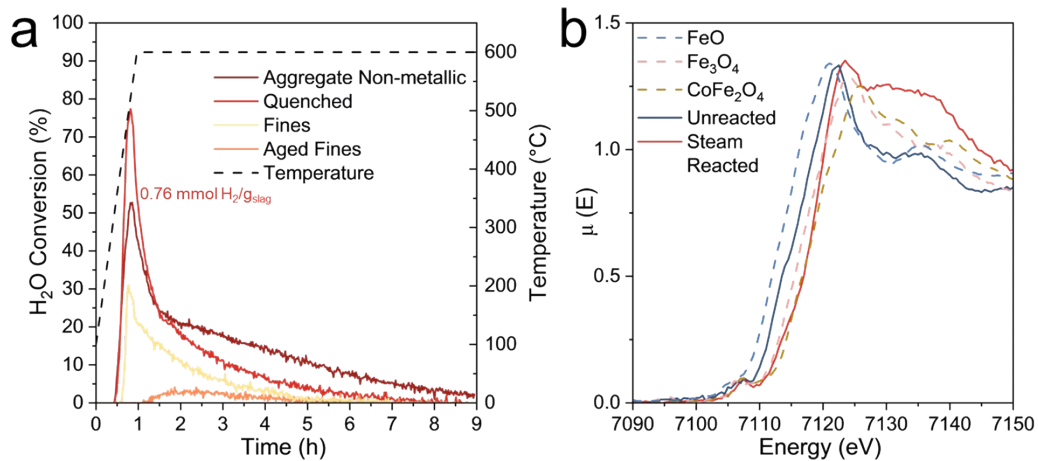


**Fig. S3** (a) H<sub>2</sub> production from water (H<sub>2</sub>O) with BOF steel slags. Experiments conducted with 6 g steel slag at 600°C and 2 sccm H<sub>2</sub>O mixed with 98 sccm Argon (Ar). Aggregate non-metallic slag is typically recycled for reuse in the blast furnace. Quenched slag was scooped directly out of the BOF. Slag fines are unrecyclable waste from the BOF. Aged fines are also the unrecyclable waste but aged outside for an unknown period. (f) X-ray absorption near edge structure (XANES) for Iron (Fe) K-edge showing the Fe oxidation in quenched slag after reacting with H<sub>2</sub>O to produce H<sub>2</sub>.

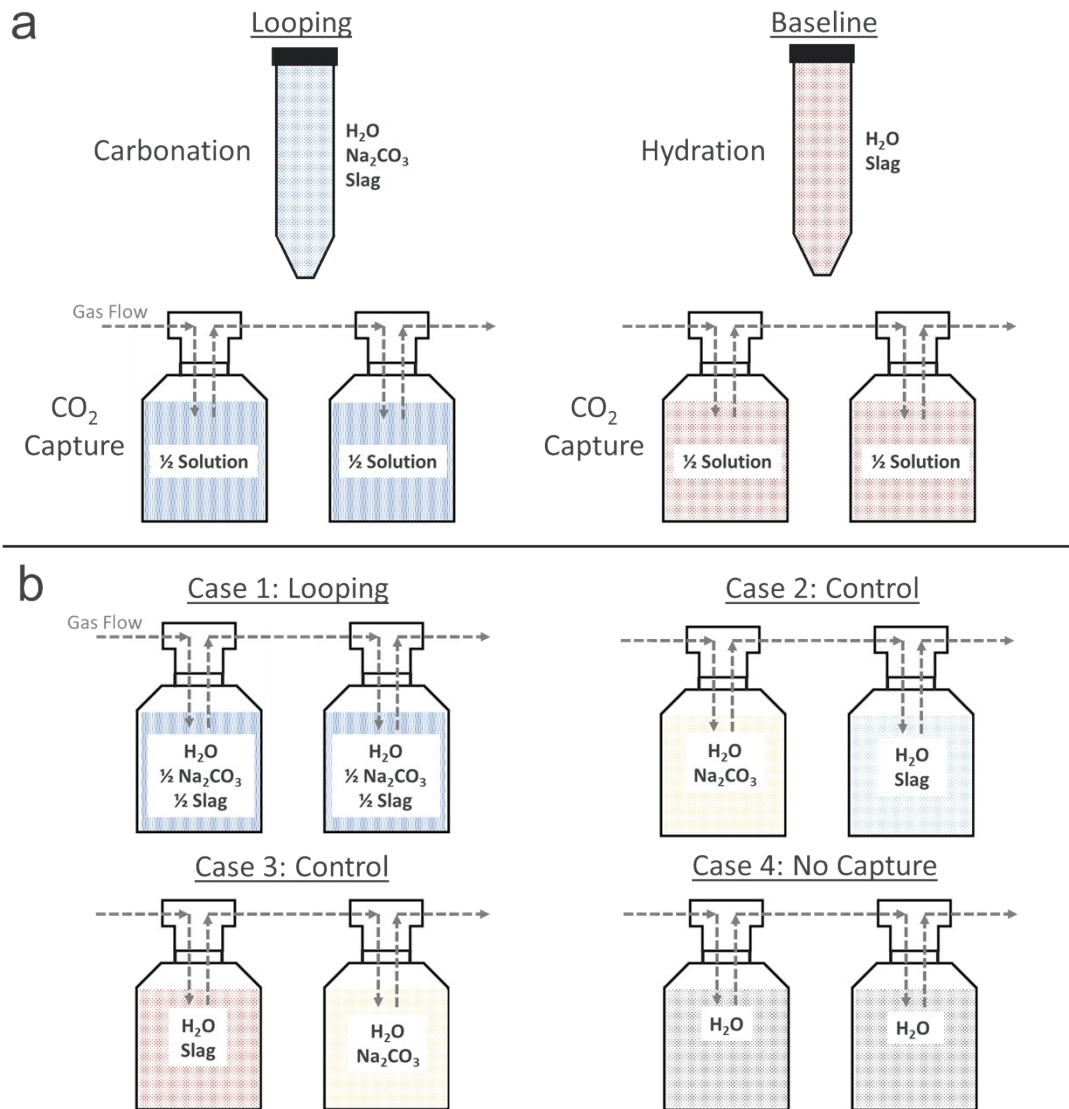


**Fig. S4** (a) Na<sub>2</sub>CO<sub>3</sub> Looping Performance “looping” and “baseline” experimental scenarios. (b) Four experimental scenarios for mechanism testing: looping, controls, and blank run.

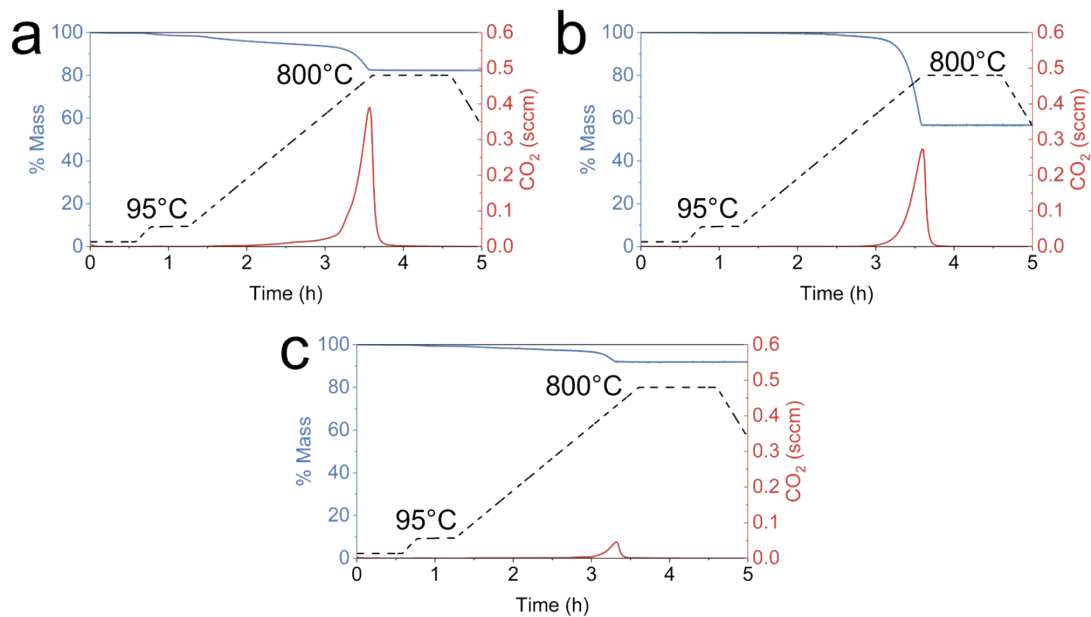


**Fig. S5** (a) Thermogravimetric analysis (TGA) and CO<sub>2</sub> evolution of carbonate-rich product from the 4<sup>th</sup> cycle of sodium carbonate looping capturing 4% CO<sub>2</sub> (Fig. 2a). (b) TGA and CO<sub>2</sub> evolution of precipitated CaCO<sub>3</sub> from the 4<sup>th</sup> cycle of the baseline experiment capturing 4% CO<sub>2</sub> (Fig. 2a). (c) TGA and CO<sub>2</sub> evolution of carbonate-rich product from the 4<sup>th</sup> cycle of air CO<sub>2</sub> sodium carbonate looping (Fig. 2e).

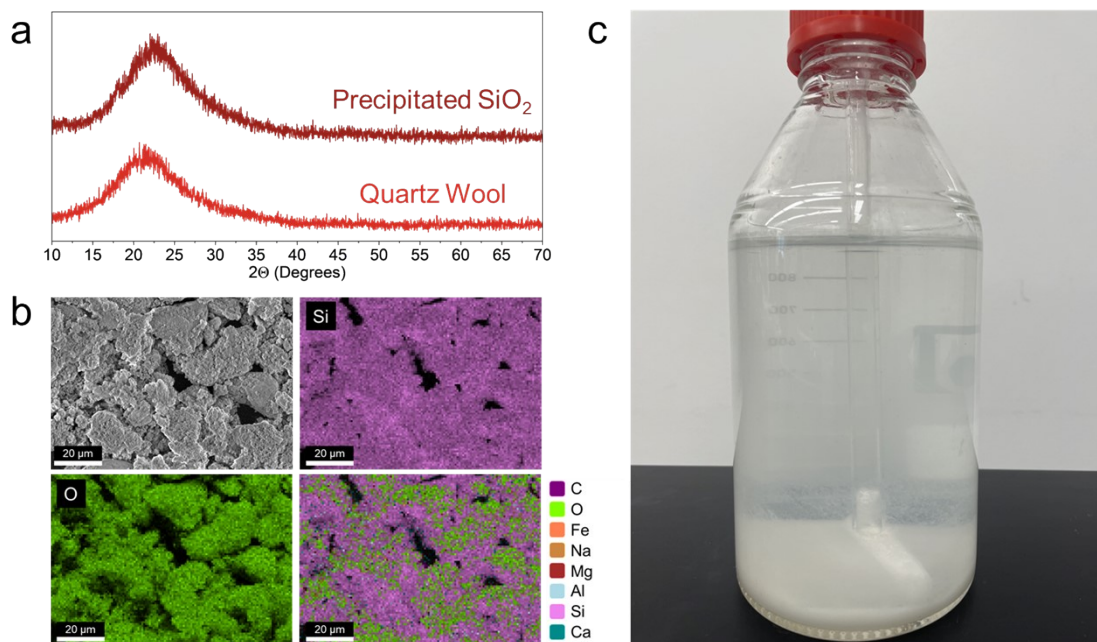


**Fig. S6** (a) XRD of amorphous precipitated SiO<sub>2</sub> compared to quartz wool as a reference. (b) SEM and EDS of precipitated SiO<sub>2</sub> showing main composition is silicon and oxygen. Sample preparation was done with 19 g of quenched BOF slag carbonated in an aqueous solution of 47 g of Na<sub>2</sub>CO<sub>3</sub> in 900 mL DI H<sub>2</sub>O for 12 hours at 60°C and 80 rpm. The mixture was then filtered, and the solution was subject to 48 hours of 90 sccm pure CO<sub>2</sub> to precipitate silicic acid which was washed, filtered and dried to produce SiO<sub>2</sub>. (c) White silicic acid gel precipitating out of solution after 48 hours of pure CO<sub>2</sub> flow.

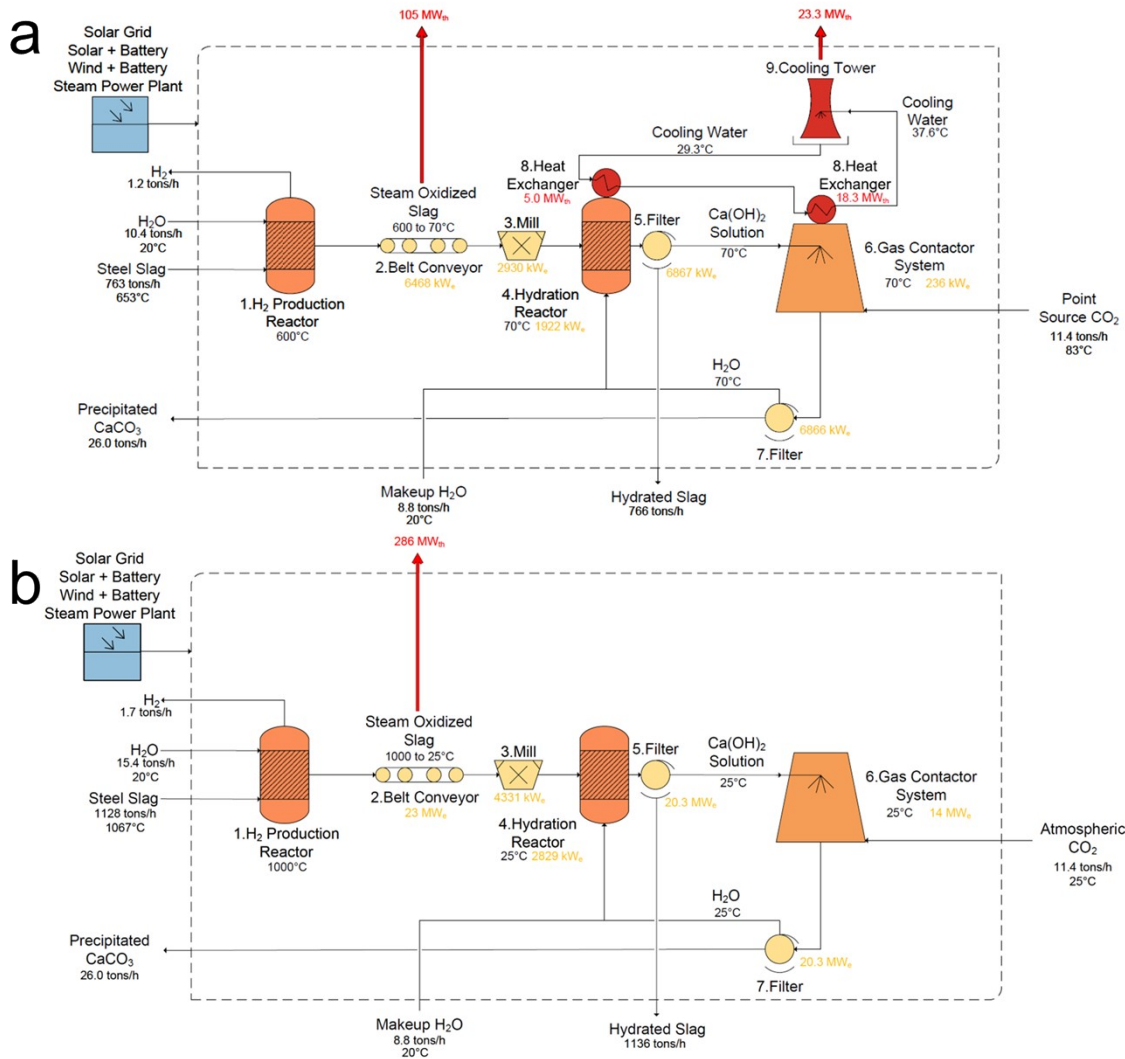


**Fig. S7** Proposed plant design for hydrogen production and CO<sub>2</sub> capture and mineralization with BOF steel slag through baseline process with a) Point-source CO<sub>2</sub> and b) air CO<sub>2</sub>.

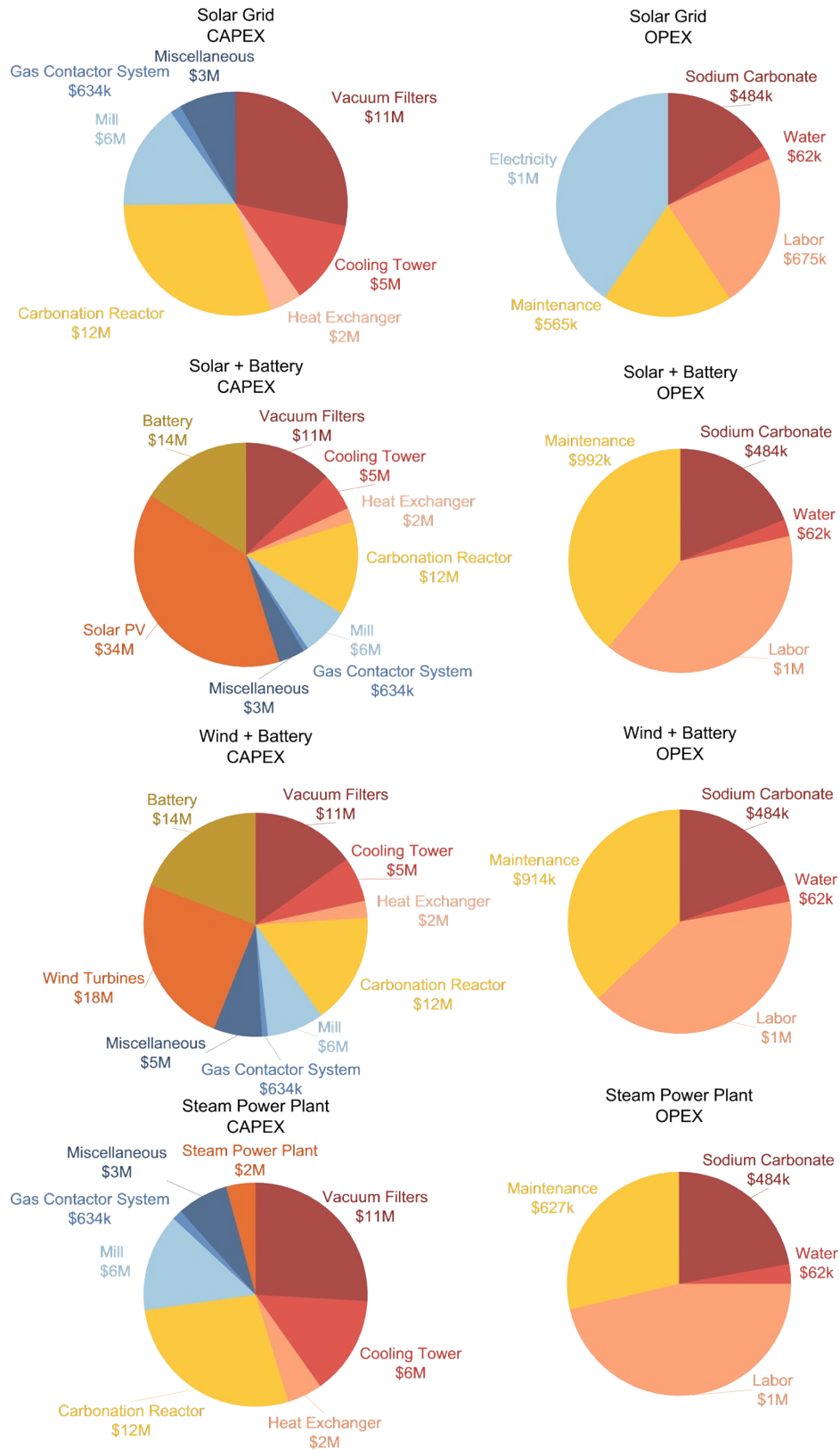
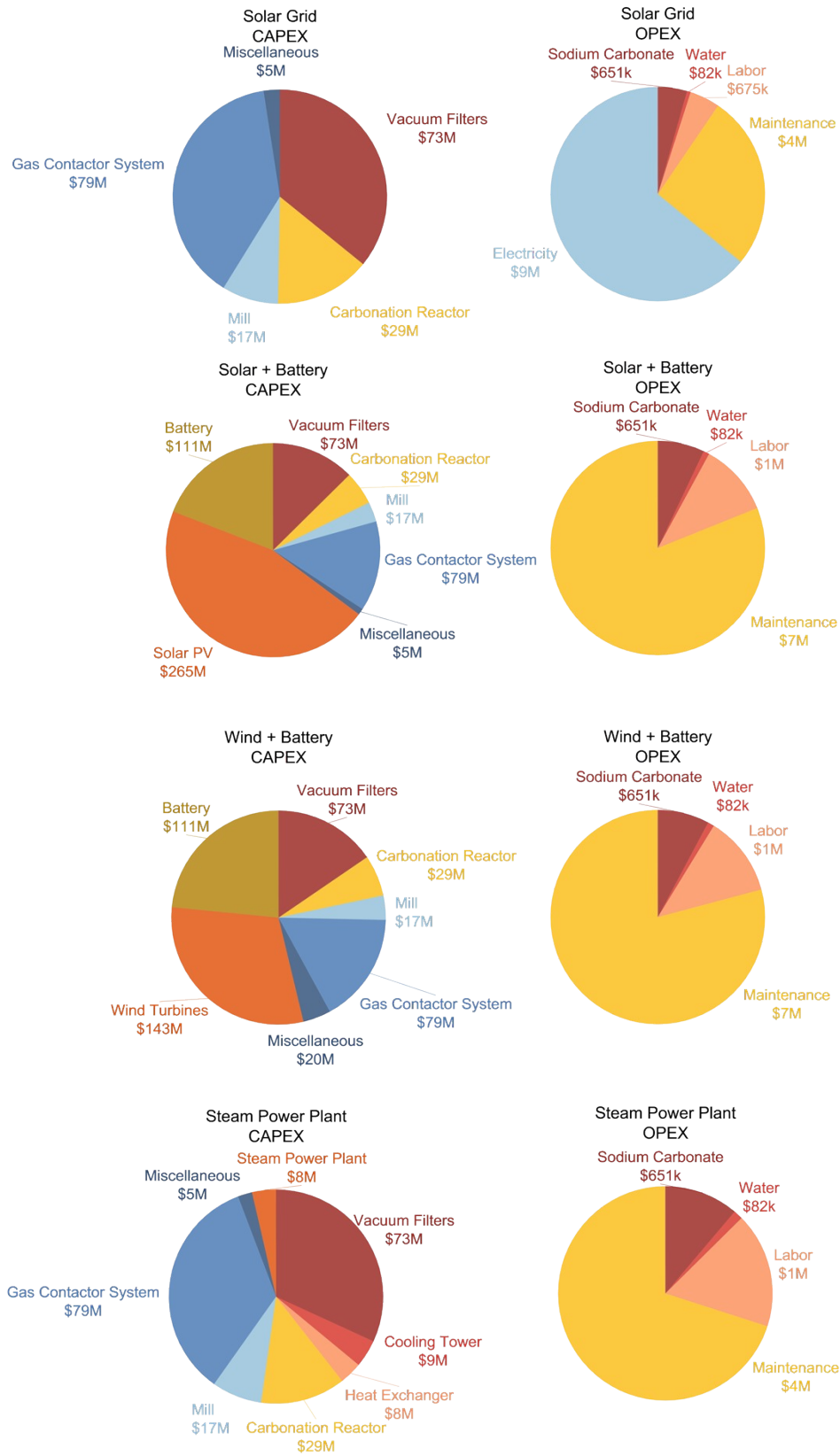
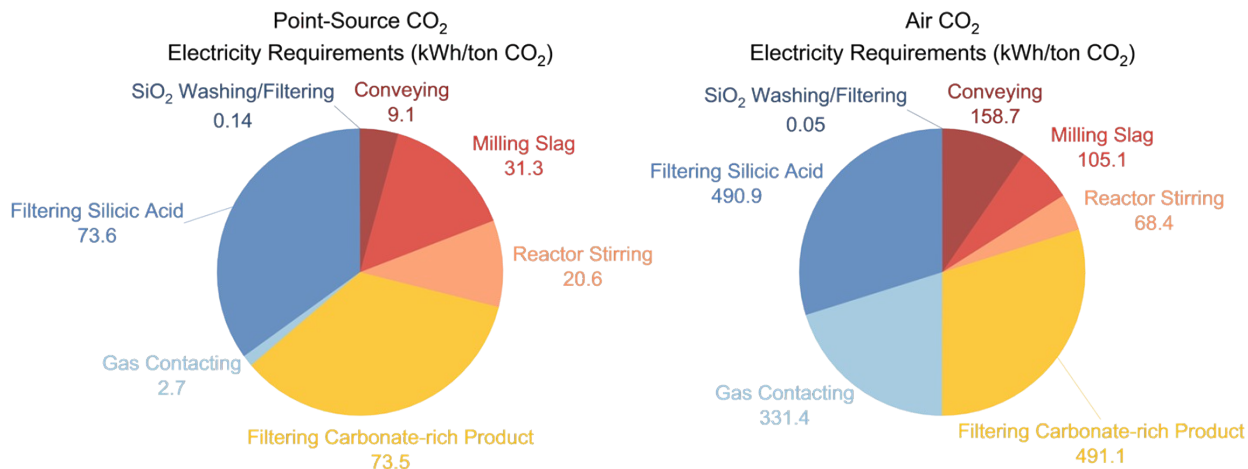


Fig. S8 Point-source  $\text{Na}_2\text{CO}_3$  looping CAPEX and OPEX for different electricity sources.



**Fig. S9** Air CO<sub>2</sub> Na<sub>2</sub>CO<sub>3</sub> looping CAPEX and OPEX for different electricity sources.



**Fig. S10** Point-source and air CO<sub>2</sub> Na<sub>2</sub>CO<sub>3</sub> looping electrical energy requirements.

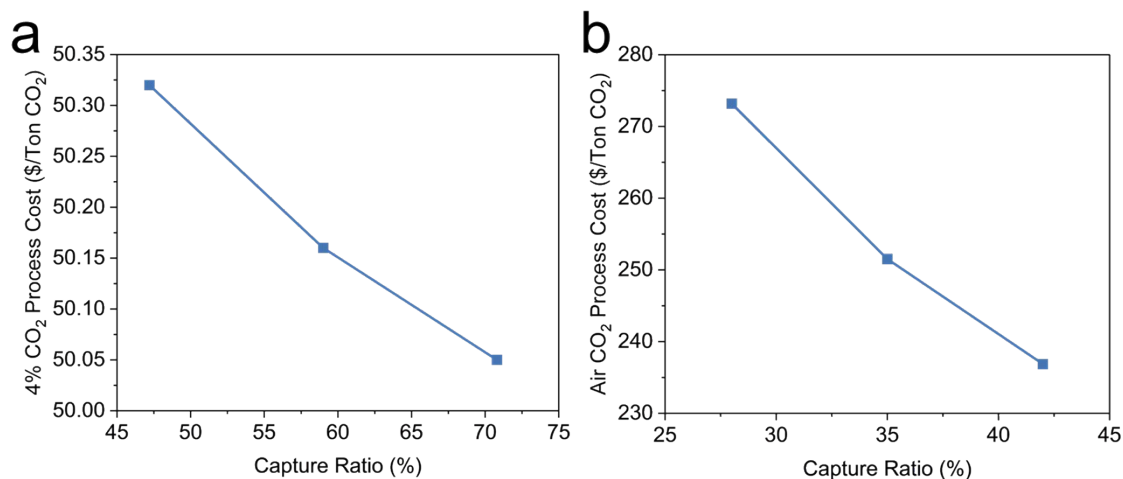


**Fig. S11** Sensitivity of process cost to the CO<sub>2</sub> capture ratio for (a) point-source and (b) air looping. Costs were evaluated by varying the CO<sub>2</sub> capture ratio by  $\pm 20\%$  relative to our experimentally observed values for each case, assuming a solar-grid electricity scenario in the scale-up analysis.

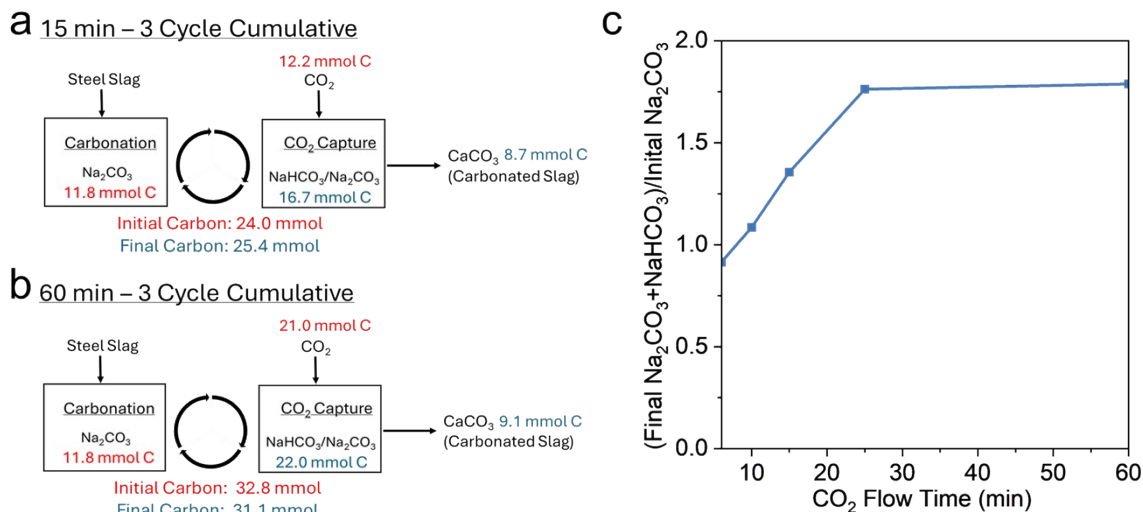


**Fig. S12** Carbon balance over 3 sodium carbonate looping cycles of (a) 15-minute and (b) 60-minute point-source CO<sub>2</sub> capture with quenched BOF slag at 45°C. 0.5 g of steel slag per cycle with 90 sccm 20% CO<sub>2</sub>/Ar. (c) Ratio of final Na<sub>2</sub>CO<sub>3</sub> and NaHCO<sub>3</sub> in solution to initial Na<sub>2</sub>CO<sub>3</sub> when CO<sub>2</sub> capture step duration is varied. To quantify the Na<sub>2</sub>CO<sub>3</sub> and NaHCO<sub>3</sub> in the solution, the pH was raised above 12.5 using sodium hydroxide (NaOH) to convert any bicarbonate (NaHCO<sub>3</sub>) into carbonate (Na<sub>2</sub>CO<sub>3</sub>). Calcium chloride (CaCl<sub>2</sub>) was then added to the solution, causing calcium carbonate (CaCO<sub>3</sub>) to precipitate. The solution was filtered, and the precipitate was dried at 100°C. The amount of CaCO<sub>3</sub> was quantified using Thermogravimetric Analysis (TGA) and Gas Chromatography (GC) by heating to 800°C to decompose CaCO<sub>3</sub> into CaO and CO<sub>2</sub>, which enabled the determination of the bicarbonate/carbonate in the solution.

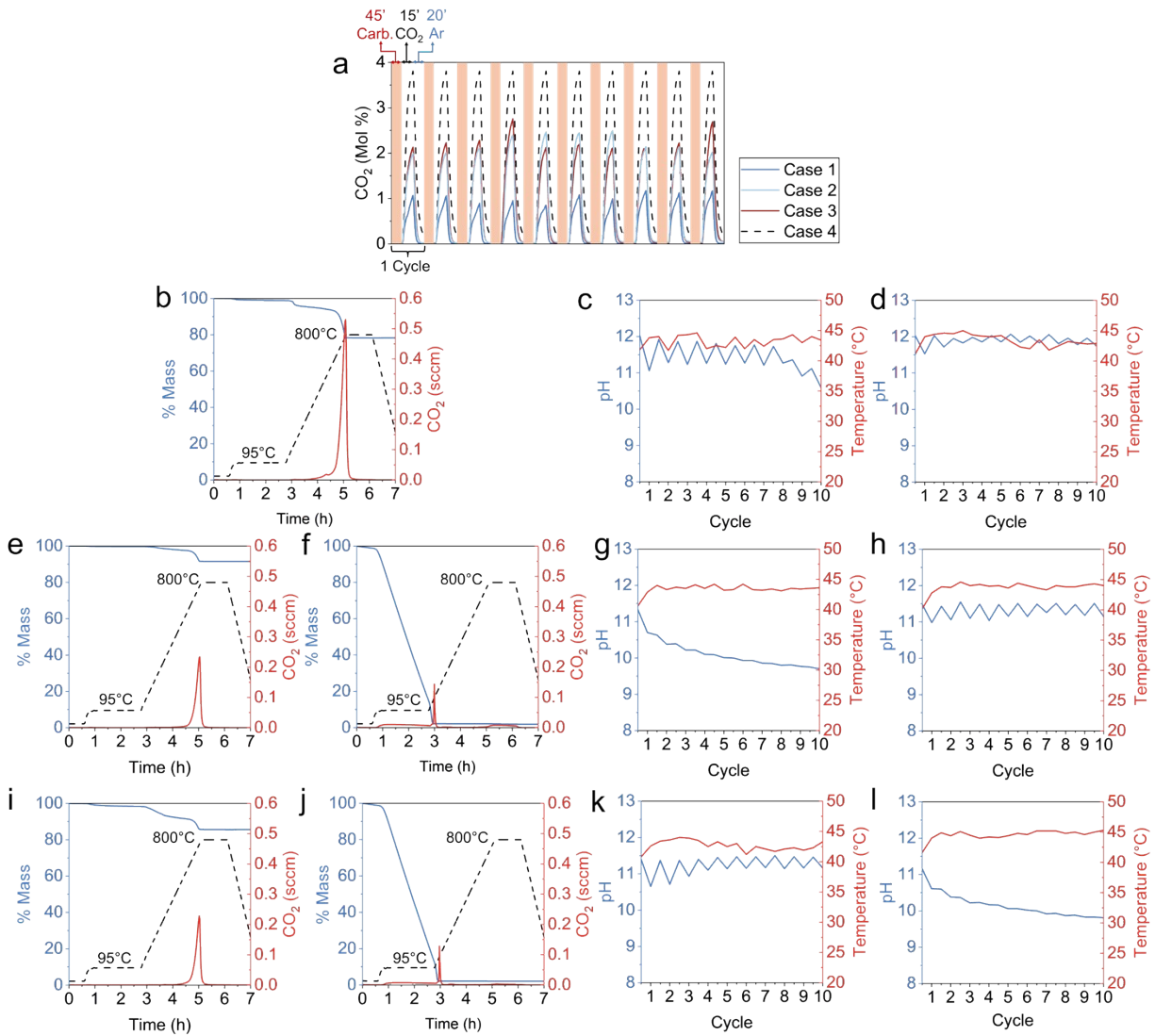


**Fig. S13** (a) 10 cycles of Case 1-4 point-source CO<sub>2</sub> capture with quenched BOF slag at 45°C. 0.5 g of steel slag per cycle with 90 sccm 4% CO<sub>2</sub>/Ar. Cases are illustrated by Fig. S4b. (b) Thermogravimetric analysis (TGA) and CO<sub>2</sub> evolution of carbonate-rich product from Case 1 sodium carbonate looping capturing 4% CO<sub>2</sub>. (c) pH and temperature in the first bottle of Case 1. Each half cycle is after carbonation, and each full cycle is after CO<sub>2</sub> capture. (d) pH and temperature in the second bottle of Case 1. (e) TGA and CO<sub>2</sub> evolution of carbonate-rich product from Case 2 control. (f) TGA and CO<sub>2</sub> evolution of Na<sub>2</sub>CO<sub>3</sub>/NaHCO<sub>3</sub> solution from first bottle in Case 2. pH and temperature in the first (g) and second (h) bottle of Case 2. (i) TGA and CO<sub>2</sub> evolution of carbonate-rich product from Case 3 control. (j) TGA and CO<sub>2</sub> evolution of Na<sub>2</sub>CO<sub>3</sub>/NaHCO<sub>3</sub> solution from second bottle in Case 3. pH and temperature in the first (k) and second (l) bottle of Case 3.

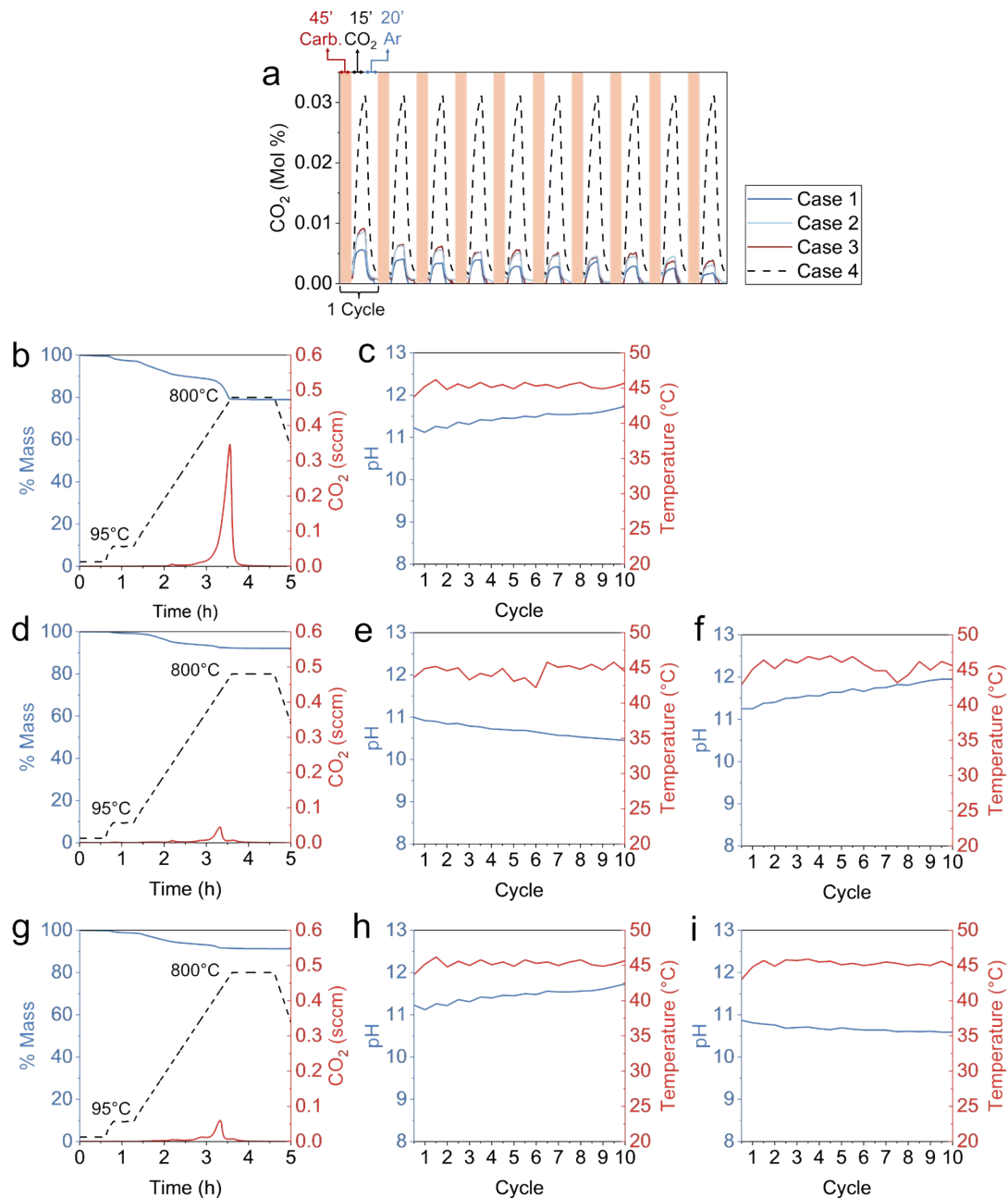


**Fig. S14** (a) 10 cycles of Case 1-4 using air with quenched BOF slag at 45°C. 0.05 g of steel slag per cycle with 90 sccm of 343 ppm CO<sub>2</sub>/Air. (b) Thermogravimetric analysis (TGA) and CO<sub>2</sub> evolution of carbonate-rich product from Case 1 sodium carbonate looping capturing 343 ppm CO<sub>2</sub>. (c) pH and temperature in the first bottle of Case 1. Each half cycle is after carbonation, and each full cycle is after CO<sub>2</sub> capture. (d) TGA and CO<sub>2</sub> evolution of carbonate-rich product from Case 2 control. pH and temperature in the first (e) and second (f) bottle of Case 2. (g) TGA and CO<sub>2</sub> evolution of carbonate-rich product from Case 3 control. pH and temperature in the first (h) and second (i) bottle of Case 3.

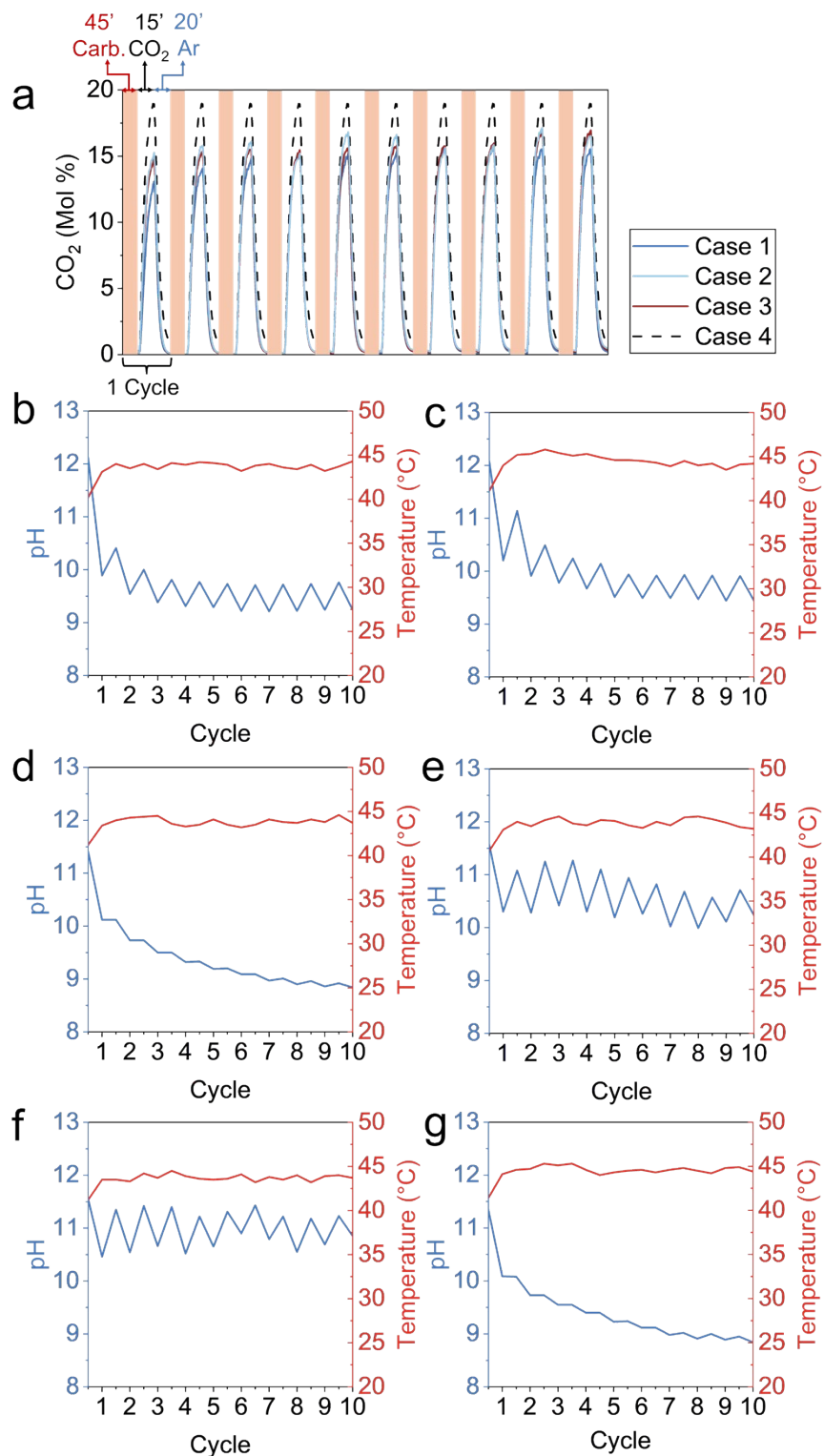


**Fig. S15** (a) 10 cycles of Case 1-4 point-source CO<sub>2</sub> capture with quenched BOF slag at 45°C. 0.5 g of steel slag per cycle with 90 sccm 20% CO<sub>2</sub>/Ar. pH and temperature in the first (b) and second (c) bottle of Case 1. pH and temperature in the first (d) and second (e) bottle of Case 2. pH and temperature in the first (f) and second (g) bottle of Case 3.

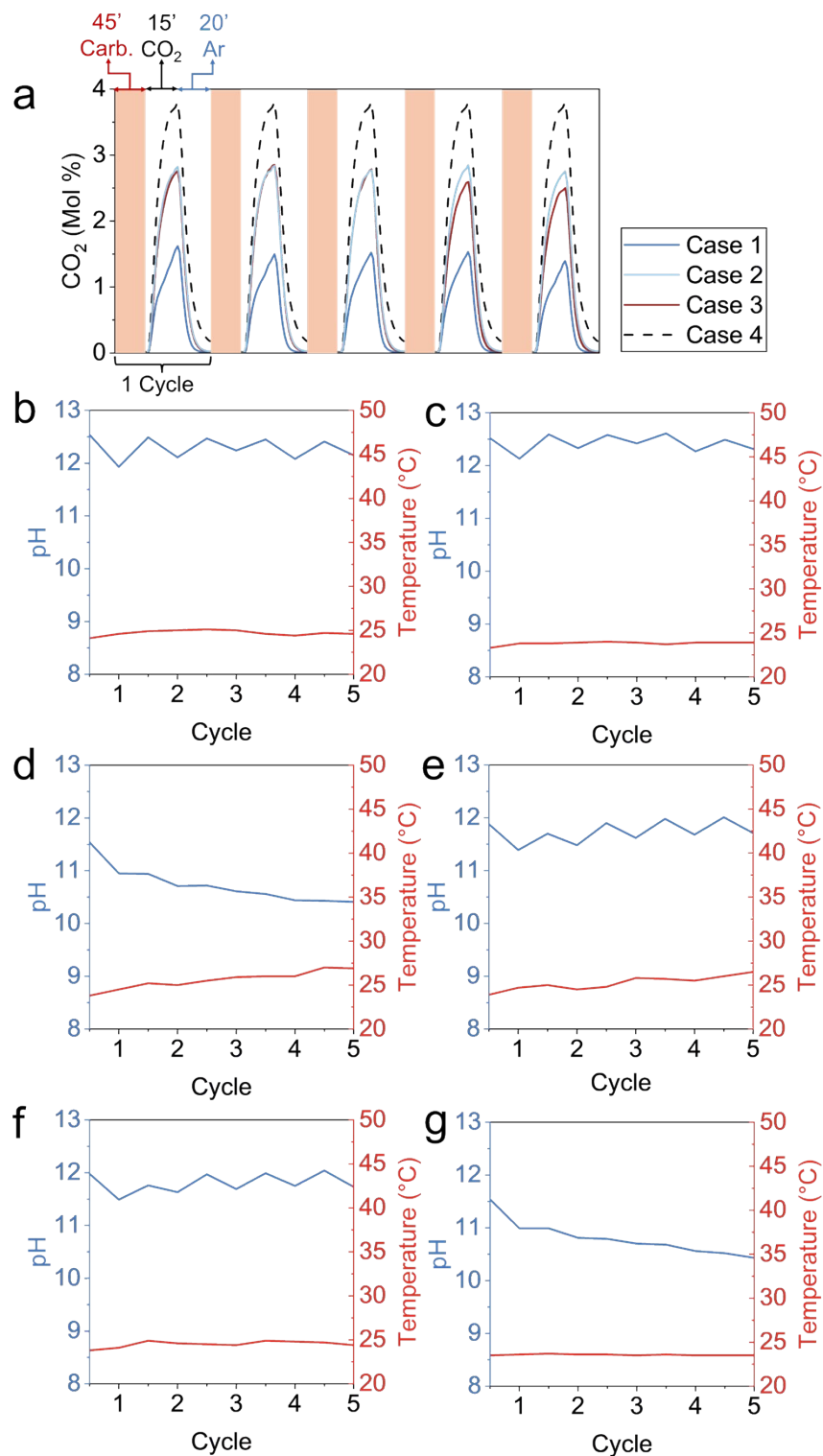


**Fig. S16** (a) 5 cycles of Case 1-4 point-source CO<sub>2</sub> capture with quenched BOF slag at 24°C. 0.5 g of steel slag per cycle with 90 sccm 4% CO<sub>2</sub>/Ar. pH and temperature in the first (b) and second (c) bottle of Case 1. pH and temperature in the first (d) and second (e) bottle of Case 2. pH and temperature in the first (f) and second (g) bottle of Case 3.

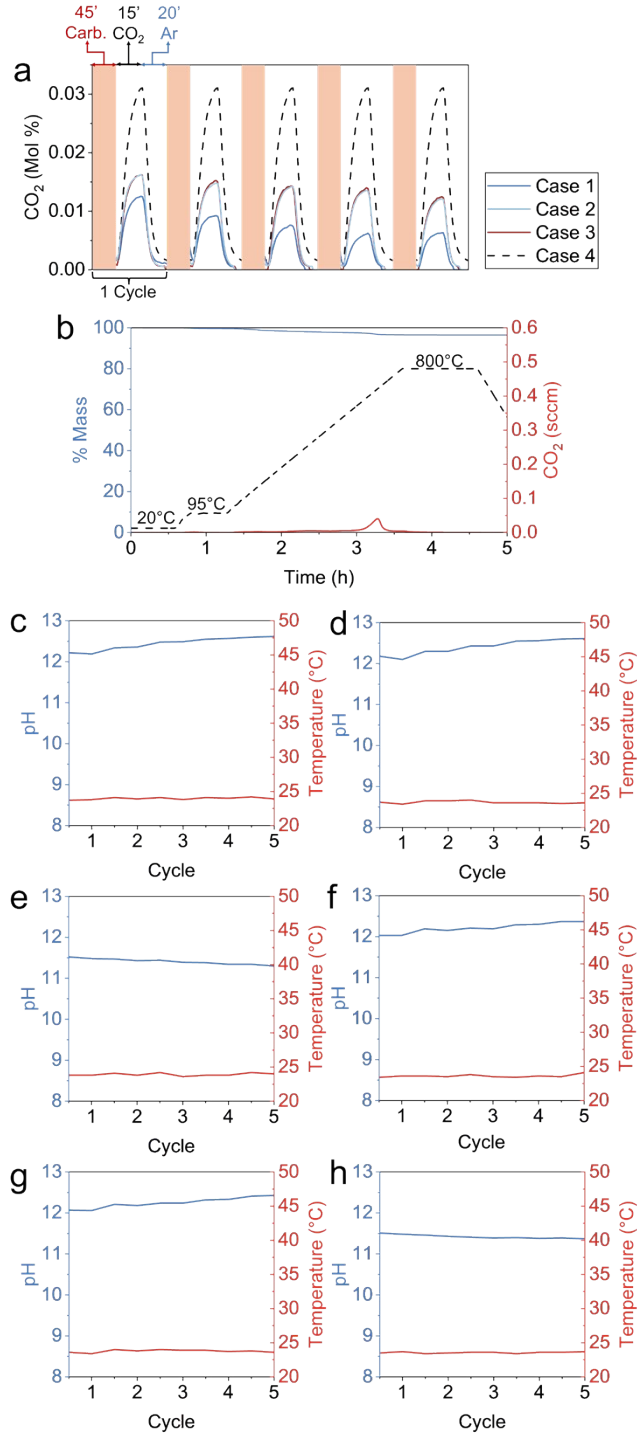


**Fig. S17** (a) 5 cycles of Case 1-4 using air with quenched BOF slag at 24°C. 0.05 g of steel slag per cycle with 90 sccm of 343 ppm CO<sub>2</sub>/Air. (b) Thermogravimetric analysis (TGA) and CO<sub>2</sub> evolution of carbonate-rich product from Case 3. pH and temperature in the first (c) and second (d) bottle of Case 1. pH and temperature in the first (e) and second (f) bottle of Case 2. pH and temperature in the first (g) and second (h) bottle of Case 3.

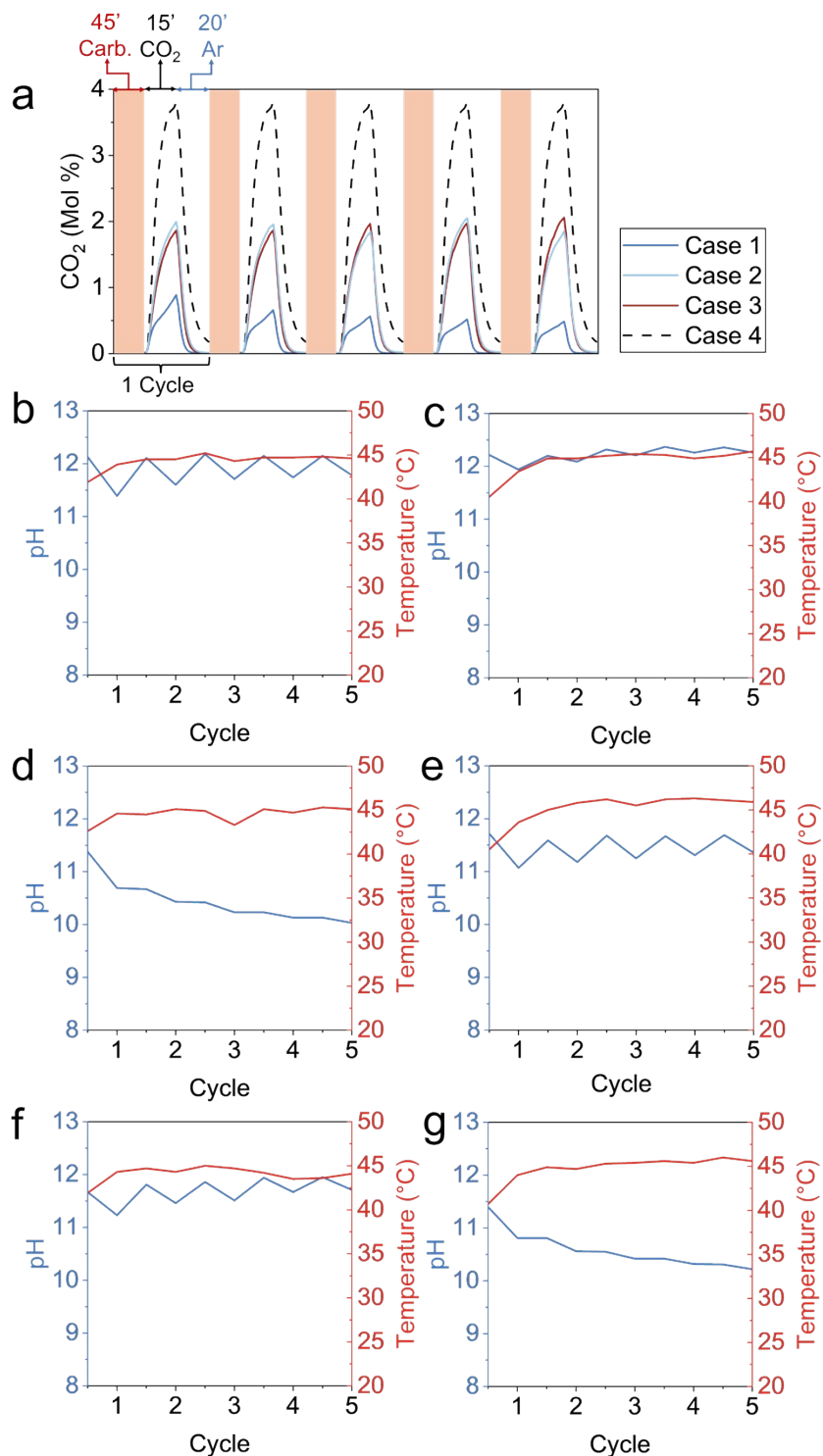


**Fig. S18** (a) 5 cycles of Case 1-4 point-source CO<sub>2</sub> capture with quenched BOF slag at 45°C with no H<sub>2</sub> production step beforehand. 0.5 g of steel slag per cycle with 90 sccm 4% CO<sub>2</sub>/Ar. pH and temperature in the first (b) and second (c) bottle of Case 1. pH and temperature in the first (d) and second (e) bottle of Case 2. pH and temperature in the first (f) and second (g) bottle of Case 3.

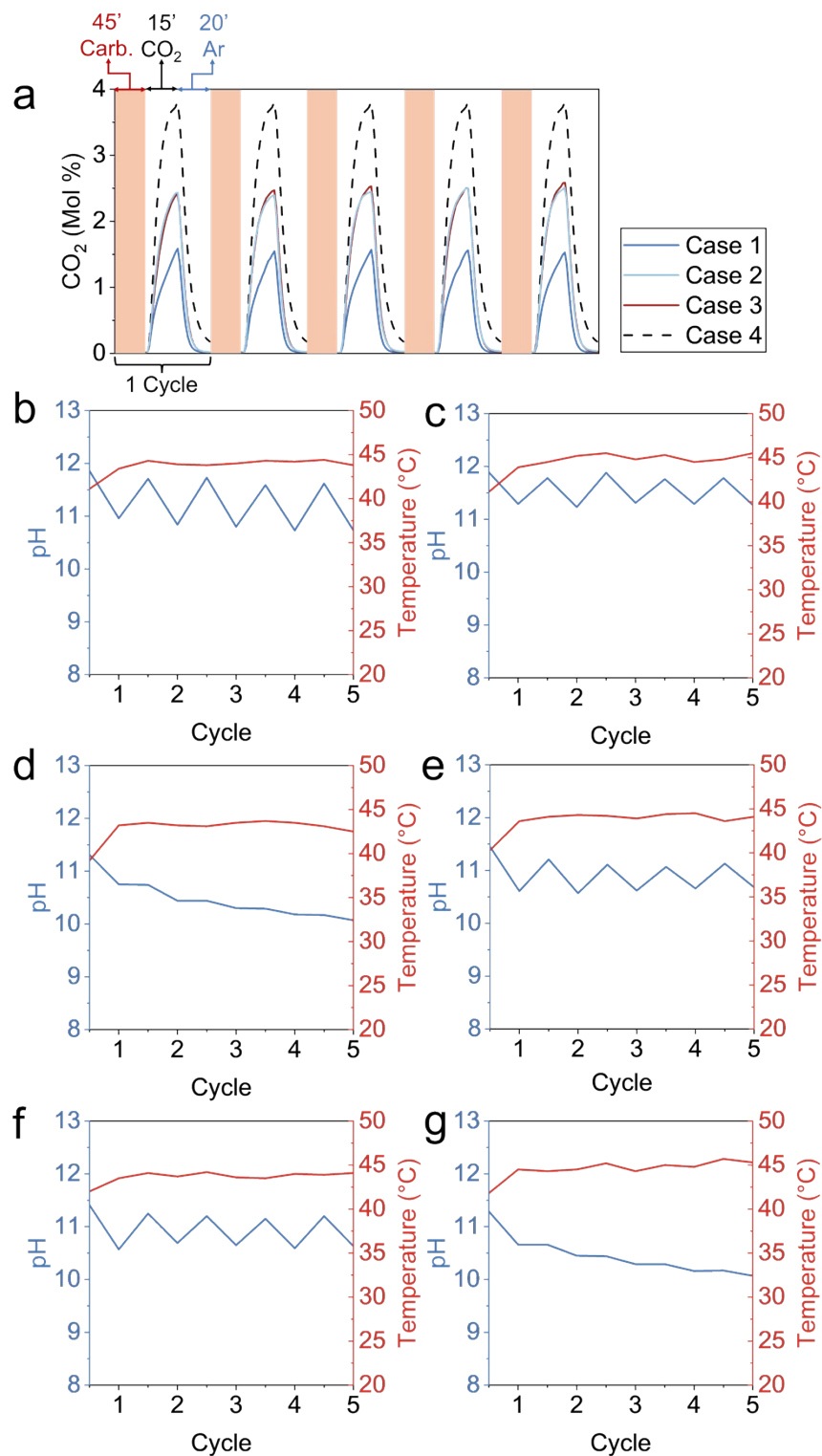


**Fig. S19** (a) 5 cycles of Case 1-4 point-source CO<sub>2</sub> capture with slag fines at 45°C. 0.5 g of steel slag per cycle with 90 sccm 4% CO<sub>2</sub>/Ar. pH and temperature in the first (b) and second (c) bottle of Case 1. pH and temperature in the first (d) and second (e) bottle of Case 2. pH and temperature in the first (f) and second (g) bottle of Case 3.

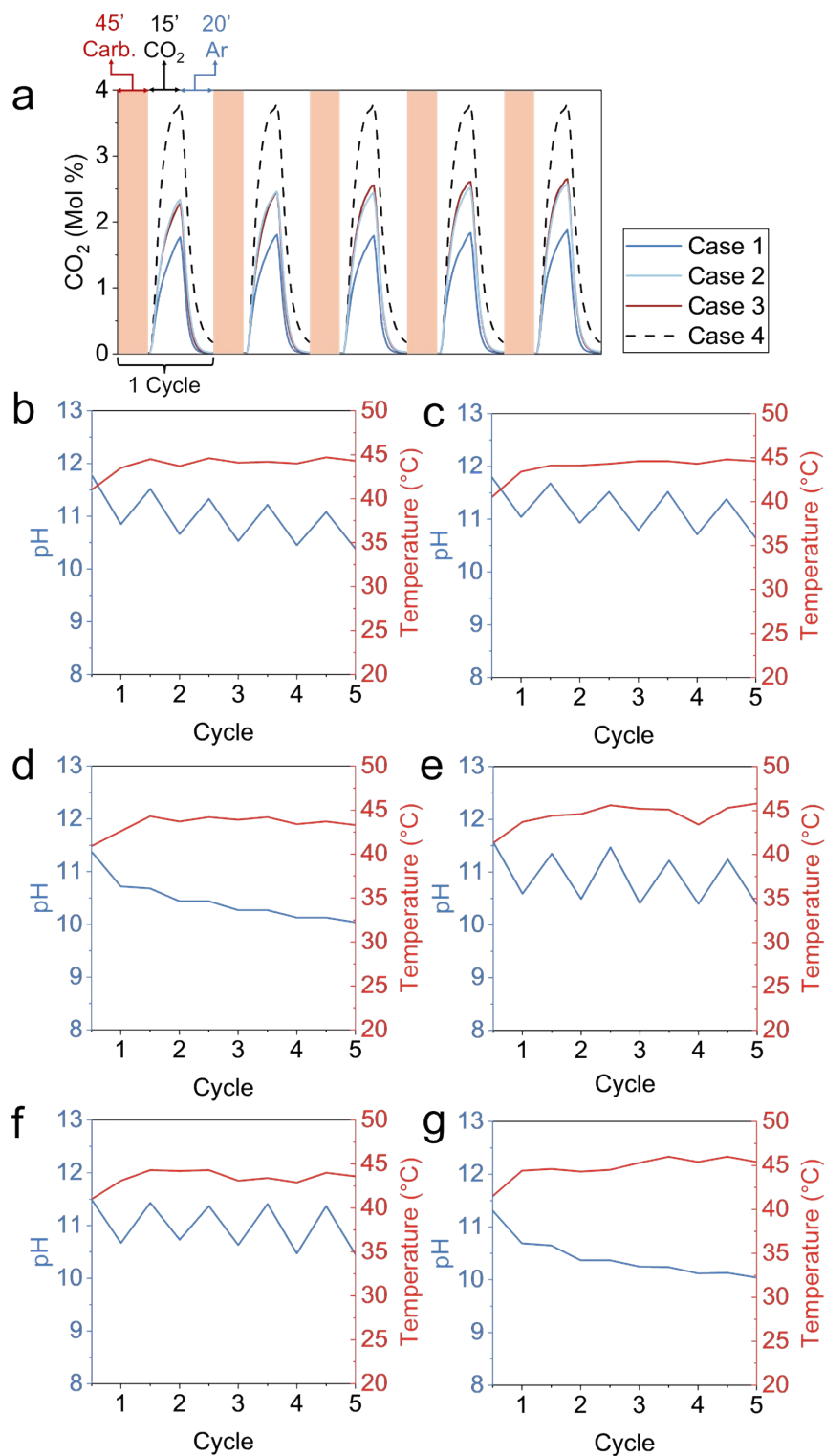


**Fig. S20** (a) 5 cycles of Case 1-4 point-source CO<sub>2</sub> capture with aged fines at 45°C. 0.5 g of steel slag per cycle with 90 sccm 4% CO<sub>2</sub>/Ar. pH and temperature in the first (b) and second (c) bottle of Case 1. pH and temperature in the first (d) and second (e) bottle of Case 2. pH and temperature in the first (f) and second (g) bottle of Case 3.

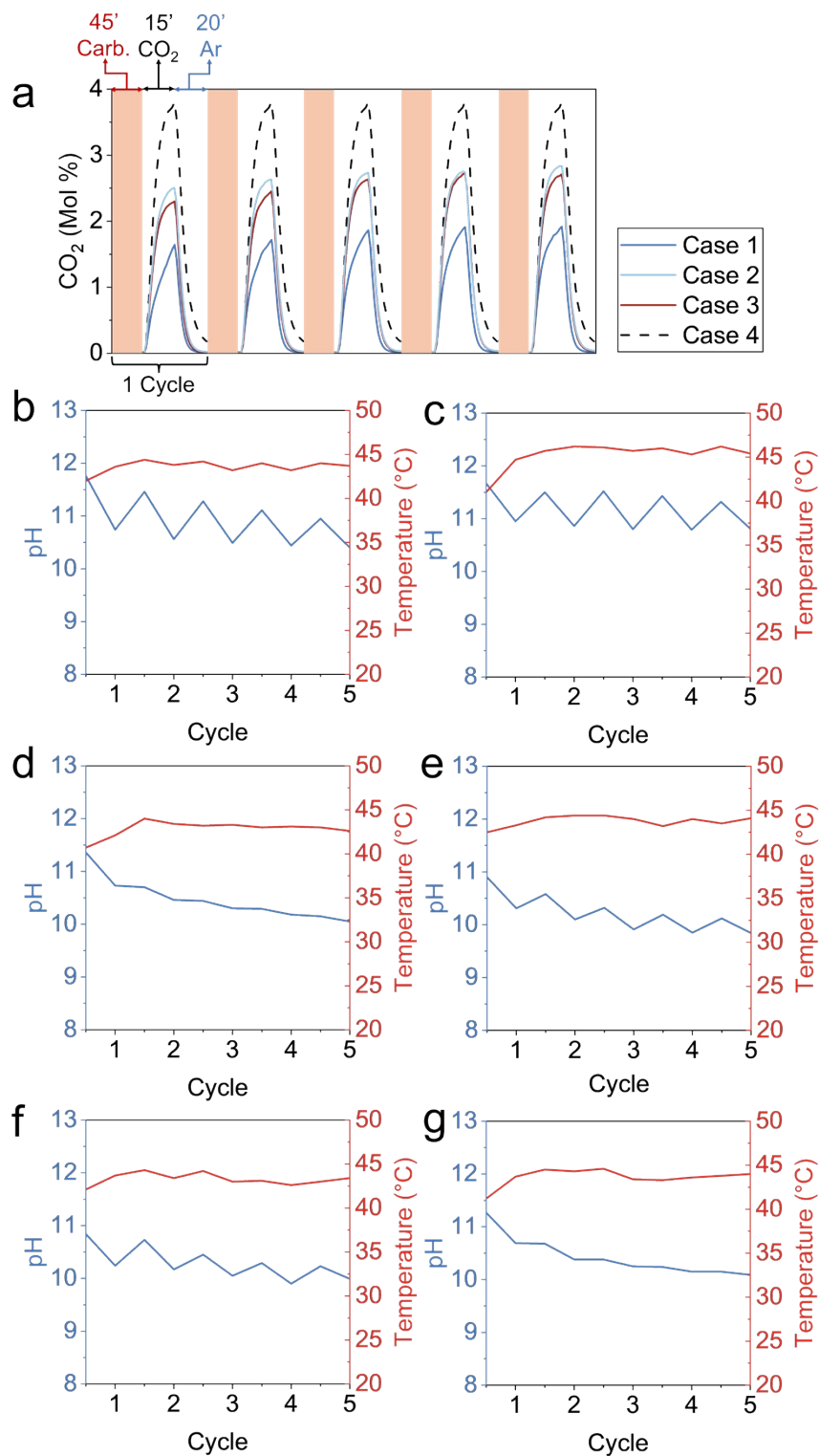


**Fig. S21** (a) 5 cycles of Case 1-4 point-source CO<sub>2</sub> capture with aggregate non-metallic BOF slag at 45°C. 0.5 g of steel slag per cycle with 90 sccm 4% CO<sub>2</sub>/Ar. pH and temperature in the first (b) and second (c) bottle of Case 1. pH and temperature in the first (d) and second (e) bottle of Case 2. pH and temperature in the first (f) and second (g) bottle of Case 3.

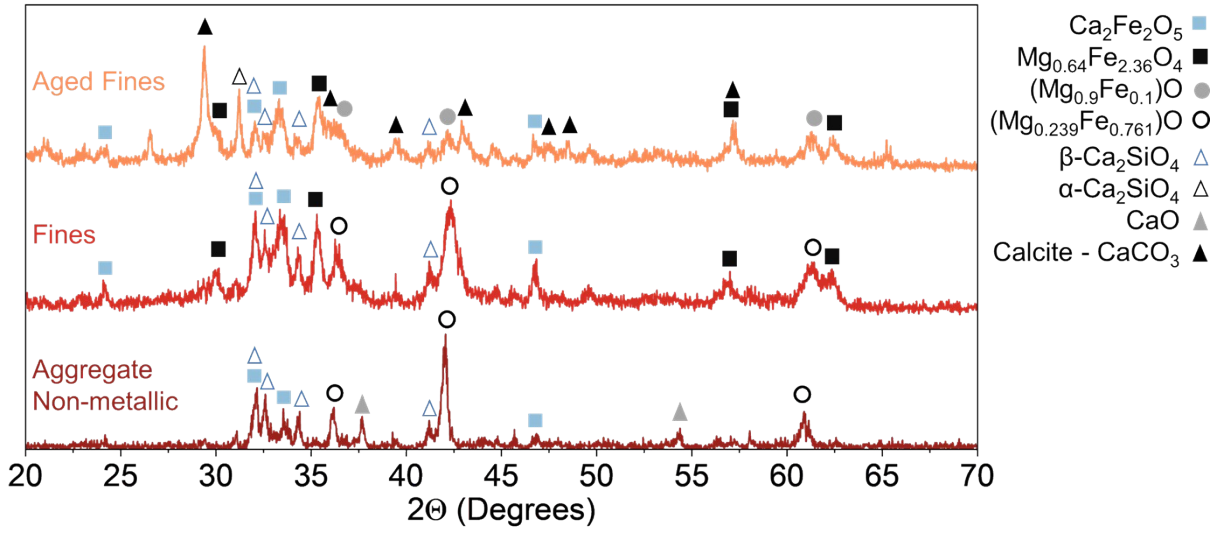


**Fig. S22** XRD of aggregate non-metallic, fines, and aged fines BOF steel slags with phase identification.

**Table S1** ICP-OES analysis of quenched steel slag.

Element	Ca	Si	Fe	Al	Mg
Mass %	41.00	27.30	15.23	2.76	10

**Table S2** ICP-OES analysis of amorphous SiO<sub>2</sub>.

Element	Ca	Fe	Al	Mg	Na
Mass %	0.59	0	2.7	0	0

**Table S3** Quenched BOF steel slag phases determined by XRD refinement.

Phase	Content (wt%)
CaO	12.45
Ca <sub>2</sub> Fe <sub>2</sub> O <sub>5</sub>	8.64
Ca <sub>2</sub> SiO <sub>4</sub>	17.04
Ca <sub>3</sub> SiO <sub>5</sub>	21.96
Mg <sub>0.8</sub> Fe <sub>0.2</sub> O	39.91

**Table S4** Calculated actively reacted phases per gram of quenched steel slag (mol/g-slag)

Phase	Point-Source Looping	Point-Source Baseline	Air CO <sub>2</sub> Looping	Air CO <sub>2</sub> Baseline
Ca <sub>3</sub> SiO <sub>5</sub>	0.000379	0.00007866	0.0001127	0.0000532
Ca <sub>2</sub> SiO <sub>4</sub>	0.00039	0.00008091	0.0001159	0.0000547
CaO	0.000874	0.00018156	0.0002601	0.0001228

**Table S5** Process mass balance (tons/h) for annually 100,000 tons of CO<sub>2</sub> captured and mineralized. Inlet steel slag components labeled with “\*”. Outlet carbonate-rich product components labeled with “#”. Outlet hydrated slag components labeled with “+”.

Na <sub>2</sub> CO <sub>3</sub> Looping			Baseline		
Component	Point-Source	Air	Component	Point-Source	Air
Inlet Flow			Inlet Flow		
Steel Slag	92.97	312.51	Steel Slag	762.90	1127.76
<i>FeO</i> *	15.19	51.06	<i>FeO</i> *	124.65	184.27
<i>Ca<sub>3</sub>SiO<sub>5</sub></i> *	8.04	8.04	<i>Ca<sub>3</sub>SiO<sub>5</sub></i> *	13.70	13.70
<i>Ca<sub>2</sub>SiO<sub>4</sub></i> *	6.24	6.24	<i>Ca<sub>2</sub>SiO<sub>4</sub></i> *	10.63	10.63
<i>CaO</i> *	4.56	4.56	<i>CaO</i> *	7.77	7.77
<i>Inactive slag</i> *	58.94	242.61	<i>Inactive slag</i> *	606.15	911.39
H <sub>2</sub> O(g) (Step 1)	1.27	4.27	H <sub>2</sub> O(g) (Step 1)	10.42	15.40
CO <sub>2</sub>	11.42	11.42	CO <sub>2</sub>	11.42	11.42
H <sub>2</sub> O(l) (SiO <sub>2</sub> Wash In)	6.44	6.44	Makeup H <sub>2</sub> O	8.77	8.77
Intermediate Flow			Intermediate Flow		
Na <sub>2</sub> CO <sub>3</sub>	232.42	312.51	Ca(OH) <sub>2</sub>	19.22	19.22
H <sub>2</sub> O(l) (Step 2/3)	4648.47	31251.18	H <sub>2</sub> O(l) (Step 2/3)	38144.82	112776.00
Na <sub>2</sub> SiO <sub>3</sub>	8.72	8.72	Product Flow		
NaOH	15.03	15.03	H <sub>2</sub>	1.17	1.72
H <sub>2</sub> SiO <sub>3</sub>	5.58	5.58	Hydrated Slag	766.38	1135.67
H <sub>2</sub> O(g) (Step 4)	1.29	1.29	<i>CSH</i> +	26.32	26.32
Product Flow			<i>Fe<sub>3</sub>O<sub>4</sub></i> +	133.91	197.95
H <sub>2</sub>	0.14	0.48	<i>Inactive slag</i> +	606.15	911.39
Carbonate-rich product	101.22	323.43	CaCO <sub>3</sub>	25.96	25.96
<i>Fe<sub>3</sub>O<sub>4</sub></i> #	16.32	54.85	Total Mass In/Out	793.50	1163.35
<i>CaCO<sub>3</sub></i> #	25.96	25.96			
<i>Inactive slag</i> #	58.94	242.61			
SiO <sub>2</sub>	4.29	4.29			
H <sub>2</sub> O(l) (SiO <sub>2</sub> Wash Out)	6.44	6.44			
Total Mass In/Out	112.09	334.63			

**Table S6** Real Steam Rankine cycle state values.

State	T (°C)	P (bar)	h (kJ/kg)
1-Saturated Liquid	45.82	0.1	191.83
2-Compressed Liquid	46.27	20	195.48
3-Superheated Vapor	312	20	3050.5
4-Wet Steam	45.8	0.1	2245

**Table S7** Lifespan for process equipment.

Equipment	Lifespan (years)	Equipment	Lifespan (years)
Gas Catalytic Reactor	25 <sup>1</sup>	Pressure Vessel/Open Tank	30 <sup>2</sup>
Belt Conveyor	20 <sup>3</sup>	Shell and Tube Heat Exchanger	25 <sup>4</sup>
Mills	25 <sup>5</sup>	Cooling Tower	25 <sup>4</sup>
Basin/Propeller	30	Solar PV	30 <sup>6</sup>
Filters	20 <sup>7</sup>	Wind Turbine	30 <sup>8</sup>
Pump	15 <sup>9</sup>	Battery	15 <sup>10</sup>
Gas Contactor System	30 <sup>11</sup>	Steam Turbine	50 <sup>12</sup>
Tray Dryer	25 <sup>13</sup>	Condenser	30 <sup>14</sup>

**Table S8** Cost components by category.

Cost Category	Components
<b>Labor</b>	- 2 laborers for overall process - 1 laborer for internal electricity generation (if applicable)
<b>Material Handling &amp; Processing</b>	- Belt conveyor - Mill - Filters/Vacuum - SiO <sub>2</sub> Washer
<b>Reactors</b>	- H <sub>2</sub> production reactor - Carbonation reactor/Propeller - Gas or Air Contactor System - Dryer
<b>Thermal Management</b>	- Heat exchanger - Cooling tower - Increased size for steam power plant condenser (if applicable)
<b>Land &amp; Materials</b>	- Land for processing facility - Land for electricity generation (if applicable) - Na <sub>2</sub> CO <sub>3</sub> (capital and replenishment twice annually) - Water (capital and operating costs)
<b>Maintenance</b>	- Process equipment maintenance - Electricity generation equipment maintenance (if applicable)
<b>Electricity &amp; Storage</b>	- Grid electricity (operating expense) - Equipment for on-site electricity generation (if applicable) - Battery storage system (if applicable)

**Table S9** Point-source Na<sub>2</sub>CO<sub>3</sub> looping installed cost and related factors for process equipment.

#	Cost Item	Size	Units	n	F <sub>m</sub>	F <sub>i</sub>	f <sub>i,alloy</sub>	FOB Cost	Installed Cost	Total Cost – 50 years
1	Gas Catalytic Reactor	31	m <sup>3</sup>	0.52	3.6 (316 s/s)	4	0.54	\$176,983	\$707,934	\$1,788,464
2	Belt Conveyor	1533	m	0.2	1.3 (316 s/s)	2.5	0.9	\$68,727	\$171,819	\$614,930
3	Mills, Grinding Circuit	94	Mg/h	0.65	1	1	1	\$2,406,205	\$2,406,205	\$6,078,833
4a	Basin	2349	m <sup>3</sup>	0.74	1	4	1	\$1,110,576	\$4,442,305	\$11,222,664
4b	Propeller	235	kW	0.52	1	2.5	1	\$96,147	\$240,368	\$607,245
5a	Rotary Disk Filter	435	m <sup>2</sup>	0.55	1	2.5	1	\$552,734	\$1,381,835	\$4,945,515
6	Gas Contactor System	61	m <sup>2</sup>	-	-	-	-	-	\$316,773	\$633,546
7a	Rotary Disk Filter	433	m <sup>2</sup>	0.55	1	2.5	1	\$550,761	\$1,376,903	\$4,927,865
5/7 b	Rotary Vane Vacuum Pump	1304	dm <sup>3</sup> /s	0.38	1	4	1	\$34,589	\$138,356	\$1,281,614
8	Tray Dryer	80	m <sup>2</sup>	0.56	1	2.5	1	\$37,593	\$93,982	\$237,428
9	Open Tank, Jacketed with Agitation	4.3	m <sup>3</sup>	0.53	1	2.5	1	\$32,871	\$82,177	\$207,604
10	Rotary Drum Filter, Vacuum	0.001	m <sup>2</sup>	0.45	1	2.5	1	\$82	\$204	\$730
11	Shell and Tube Heat Exchanger	395	m <sup>2</sup>	0.71	2.4 (s/s)	3.5	0.64	\$206,576	\$723,016	\$1,826,567
12	Cooling Tower	620	L/s	0.64	1	3.5	1	\$539,612	\$1,888,644	\$4,771,310
	Solar PV	2407	kW	-	-	-	-	-	\$16,941,933	\$33,883,866
	Wind Turbine	2407	kW	-	-	-	-	-	\$9,158,163	\$18,316,326
	Battery	38504	kWh	-	-	-	-	-	\$3,542,404	\$14,169,617

**Table S10** Point-source  $\text{Na}_2\text{CO}_3$  looping installed cost and related factors for process equipment within and changed by steam power cycle.

#	Cost Item	Size	Units	n	$F_m$	$F_i$	$f_{i,\text{alloy}}$	FOB Cost	Installed Cost	Total Cost – 50 years
2	Belt Conveyor	1194	m	0.2	1.3 (316 s/s)	2.5	0.9	\$60,659	\$151,647	\$542,737
11	Shell and Tube Heat Exchanger	507	m <sup>2</sup>	0.71	2.4 (s/s)	3.5	0.64	\$246,979	\$864,428	\$2,183,817
12	Cooling Tower	798	L/s	0.64	1	3.5	1	\$693,986	\$2,428,949	\$6,136,293
	Single Valve, Single Stage Steam Turbine	2407	kW	0.51	1	2.5	1	\$183,033	\$457,583	\$674,332
	Pump Centrifugal	11	kW	0.29	1.93 (316 s/s)	4	0.7	\$7,504	\$30,016	\$139,023
	Direct Contact Barometric Condenser	178	L/s	0.6	1	2.5	1	\$4,006	\$10,016	\$25,304
	Vertical Pressure Vessel	14.4	m <sup>3</sup>	0.52	2 (316 s/s)	4	0.69	\$96,876	\$387,504	\$978,956

**Table S11** Point-source baseline installed cost and related factors for process equipment.

#	Cost Item	Size	Units	n	F <sub>m</sub>	F <sub>i</sub>	f <sub>i,alloy</sub>	FOB Cost	Installed Cost	Total Cost – 50 years
1	Gas Catalytic Reactor	127	m <sup>3</sup>	0.52	3.6 (316 s/s)	4	0.54	\$368,759	\$1,475,034	\$3,726,403
2	Belt Conveyor	11687	m	0.2	1.3 (316 s/s)	2.5	0.9	\$289,126	\$722,814	\$2,586,913
3	Mills, Grinding Circuit	772	Mg/h	0.65	1	1	1	\$16,771,726	\$16,771,726	\$42,370,677
4a	Basin	19200	m <sup>3</sup>	0.74	1	4	1	\$5,257,149	\$21,028,596	\$53,124,874
4b	Propeller	1922	kW	0.52	1	2.5	1	\$786,844	\$1,967,111	\$4,969,544
5a	Rotary Disk Filter	3560	m <sup>2</sup>	0.55	1	2.5	1	\$4,528,203	\$11,320,508	\$40,515,502
6	Gas Contactor System	475	m <sup>2</sup>	-	-	-	-	-	\$2,459,157	\$4,918,314
7a	Rotary Disk Filter	3,533	m <sup>2</sup>	0.55	1	2.5	1	\$4,100,513	\$10,251,283	\$36,688,801
5/7 b	Rotary Vane Vacuum Pump	10,679	dm <sup>3</sup> /s	0.38	1	4	1	\$243,020	\$972,080	\$9,004,534
8	Shell and Tube Heat Exchanger	426	m <sup>2</sup>	0.71	2.4 (s/s)	3.5	0.64	\$218,187	\$763,654	\$1,929,232
9	Cooling Tower	670	L/s	0.64	1	3.5	1	\$582,815	\$2,039,853	\$5,153,313
	Solar PV	25289	kW	-	-	-	-	-	\$178,037,601	\$356,075,201
	Wind Turbine	25289	kW	-	-	-	-	-	\$96,240,338	\$192,480,676
	Battery	161852	kWh	-	-	-	-	-	\$37,226,044	\$148,904,175

**Table S12** Point-source baseline installed cost and related factors for process equipment within and changed by steam power cycle.

#	Cost Item	Size	Units	n	F <sub>m</sub>	F <sub>i</sub>	f <sub>i,alloy</sub>	FOB Cost	Installed Cost	Total Cost – 50 years
2	Belt Conveyor	9894	m	0.2	1.3 (316 s/s)	2.5	0.9	\$266,019	\$665,049	\$2,380,174
8	Shell and Tube Heat Exchanger	1612	m <sup>2</sup>	0.71	2.4 (s/s)	3.5	0.64	\$561,219	\$1,964,267	\$4,962,358
9	Cooling Tower	2535	L/s	0.64	1	3.5	1	\$1,577,676	\$5,521,866	\$13,949,978
	Single Valve, Single Stage Steam Turbine	25289	kW	0.51	1	2.5	1	\$1,726,514	\$4,316,285	\$6,360,841
	Pump Centrifugal	115	kW	0.29	1.93 (316 s/s)	4	0.7	\$46,572	\$186,289	\$862,814
	Direct Contact Barometric Condenser	1866	L/s	0.6	1	2.5	1	\$282,754	\$706,884	\$1,785,813
	Vertical Pressure Vessel	69.4	m <sup>3</sup>	0.52	2 (316 s/s)	4	0.69	\$219,694	\$878,774	\$2,220,061

**Table S13** Air CO<sub>2</sub> Na<sub>2</sub>CO<sub>3</sub> looping installed cost and related factors for process equipment.

#	Cost Item	Size	Units	n	F <sub>m</sub>	F <sub>i</sub>	f <sub>i,alloy</sub>	FOB Cost	Installed Cost	Total Cost – 50 years
1	Gas Catalytic Reactor	26	m <sup>3</sup>	0.52	3.6 (316 s/s)	4	0.54	\$161,680	\$646,718	\$1,633,814
2	Belt Conveyor	7988	m	0.2	1.3 (316 s/s)	2.5	0.9	\$199,962	\$499,905	\$1,789,134
3	Mills, Grinding Circuit	316	Mg/h	0.65	1	1	1	\$6,870,346	\$6,870,346	\$17,356,663
4a	Basin	7810	m <sup>3</sup>	0.74	1	4	1	\$2,701,955	\$10,807,821	\$27,303,968
4b	Propeller	781	kW	0.52	1	2.5	1	\$319,693	\$799,233	\$2,019,115
5a	Rotary Disk Filter	2883	m <sup>2</sup>	0.55	1	2.5	1	\$3,667,031	\$9,167,577	\$32,810,276
6	Gas Contactor System	7611	m <sup>2</sup>	-	-	-	-	-	\$39,420,400	\$78,840,800
7a	Rotary Disk Filter	2883	m <sup>2</sup>	0.55	1	2.5	1	\$3,667,031	\$9,167,577	\$32,810,276
5/7 b	Rotary Vane Vacuum Pump	8651	dm <sup>3</sup> /s	0.38	1	4	1	\$196,867	\$787,467	\$7,294,432
8	Tray Dryer	40	m <sup>2</sup>	0.56	1	2.5	1	\$25,499	\$63,748	\$161,048
9	Open Tank, Jacketed with Agitation	2.1	m <sup>3</sup>	0.53	1	2.5	1	\$22,765	\$56,912	\$143,777
10	Rotary Drum Filter, Vacuum	0.079	m <sup>2</sup>	0.45	1	2.5	1	\$8,153	\$20,384	\$72,952
	Solar PV	18786	kW	-	-	-	-	-	\$132,255,320	\$264,510,640
	Wind Turbine	18786	kW	-	-	-	-	-	\$71,492,183	\$142,984,366
	Battery	300580	kWh	-	-	-	-	-	\$27,653,385	\$110,613,540

**Table S14** Air CO<sub>2</sub> Na<sub>2</sub>CO<sub>3</sub> looping installed cost and related factors for process equipment within and changed by steam power cycle.

#	Cost Item	Size	Units	n	F <sub>m</sub>	F <sub>i</sub>	f <sub>i,alloy</sub>	FOB Cost	Installed Cost	Total Cost – 50 years
2	Belt Conveyor	7127	m	0.2	1.3 (316 s/s)	2.5	0.9	\$188,873	\$472,182	\$1,689,915
	Shell and Tube Heat Exchanger	2699	m <sup>2</sup>	0.71	2.4 (s/s)	3.5	0.64	\$882,609	\$3,089,131	\$7,804,122
	Cooling Tower	1385	L/s	0.64	1	3.5	1	\$1,071,719	\$3,751,016	\$9,476,251
	Single Valve, Single Stage Steam Turbine	18786	kW	0.51	1	2.5	1	\$1,282,542	\$3,206,354	\$4,725,154
	Pump Centrifugal	86	kW	0.29	1.93 (316 s/s)	4	0.7	\$34,596	\$138,385	\$640,942
	Direct Contact Barometric Condenser	1386	L/s	0.6	1	2.5	1	\$210,044	\$525,109	\$1,326,592
	Vertical Pressure Vessel	35.5	m <sup>3</sup>	0.52	2 (316 s/s)	4	0.69	\$154,946	\$619,784	\$1,565,771

**Table S15** Air CO<sub>2</sub> baseline installed cost and related factors for process equipment.

#	Cost Item	Size	Units	n	F <sub>m</sub>	F <sub>i</sub>	f <sub>i,alloy</sub>	FOB Cost	Installed Cost	Total Cost – 50 years
1	Gas Catalytic Reactor	94	m <sup>3</sup>	0.52	3.6 (316 s/s)	4	0.54	\$315,121	\$1,260,483	\$3,184,379
2	Belt Conveyor	28006	m	0.2	1.3 (316 s/s)	2.5	0.9	\$483,967	\$1,209,917	\$4,330,228
3	Mills, Grinding Circuit	1141	Mg/h	0.65	1	1	1	\$24,792,987	\$24,792,987	\$62,634,914
4a	Basin	28288	m <sup>3</sup>	0.74	1	4	1	\$7,003,258	\$28,013,034	\$70,769,769
4b	Propeller	2829	kW	0.52	1	2.5	1	\$1,157,929	\$2,894,823	\$7,313,237
5a	Rotary Disk Filter	10483	m <sup>2</sup>	0.55	1	2.5	1	\$13,335,282	\$33,338,205	\$119,315,682
6	Gas Contactor System	28040	m <sup>2</sup>	-	-	-	-	-	\$145,233,053	\$290,466,105
7a	Rotary Disk Filter	10443	m <sup>2</sup>	0.55	1	2.5	1	\$13,284,366	\$33,210,915	\$118,860,118
5/7 b	Rotary Vane Vacuum Pump	31449	dm <sup>3</sup> /s	0.38	1	4	1	\$715,679	\$2,862,717	\$26,517,802
	Solar PV	84614	kW	-	-	-	-	-	\$595,682,532	\$1,191,365,063
	Wind Turbine	84614	kW	-	-	-	-	-	\$322,003,262	\$644,006,525
	Battery	1353824	kWh	-	-	-	-	-	\$124,551,802	\$498,207,208

**Table S16** Air CO<sub>2</sub> baseline installed cost and related factors for process equipment within and changed by steam power cycle.

#	Cost Item	Size	Units	n	F <sub>m</sub>	F <sub>i</sub>	f <sub>i,alloy</sub>	FOB Cost	Installed Cost	Total Cost – 50 years
2	Belt Conveyor	25047	m	0.2	1.3 (316 s/s)	2.5	0.9	\$457,685	\$1,144,213	\$4,095,079
	Shell and Tube Heat Exchanger	9501	m <sup>2</sup>	0.71	2.4 (s/s)	3.5	0.64	\$3,106,692	\$10,873,422	\$27,469,699
	Cooling Tower	4876	L/s	0.64	1	3.5	1	\$2,398,060	\$8,393,208	\$21,203,895
	Single Valve, Single Stage Steam Turbine	66126	kW	0.51	1	2.5	1	\$4,514,414	\$11,286,034	\$16,632,050
	Pump Centrifugal	301	kW	0.29	1.93 (316 s/s)	4	0.7	\$121,775	\$487,101	\$2,256,048
	Direct Contact Barometric Condenser	4880	L/s	0.6	1	2.5	1	\$739,332	\$1,848,330	\$4,669,466
	Vertical Pressure Vessel	55.9	m <sup>3</sup>	0.52	2 (316 s/s)	4	0.69	\$196,263	\$785,052	\$1,983,289

**Table S17** Levelized cost of electricity (LCOE) for all scenarios (Units: \$/MWh). The LCOE for internal electricity sources varies across process scenarios because each scenario assumes the same labor input, which does not scale proportionally with equipment sizing. \* For the baseline air CO<sub>2</sub> scenario, additional electricity supplied by the solar grid is needed to satisfy the overall energy requirements.

Electricity Source	Point-Source Looping	Point-Source Baseline	Air CO <sub>2</sub> Looping	Air CO <sub>2</sub> Baseline
Solar Grid	58	58	58	58
Solar PV + Battery	153	138	139	137
Wind + Battery	116	101	102	100
Steam Turbine	26	8	6	19*

## ***Hydrogen Production***

H<sub>2</sub> was produced by reacting steam with BOF slags from Cleveland-Cliffs – Cleveland Works. H<sub>2</sub> production experiments were conducted using 6 grams of BOF slag at 600°C, with a mixture of 2 sccm H<sub>2</sub>O vapor and 98 sccm Ar. To determine the optimal temperature for H<sub>2</sub> production, experiments were conducted from 500 to 1000°C, revealing the highest production at 650°C (Fig. S2) demonstrating a similar trend to Li et al.<sup>15</sup> H<sub>2</sub> production is shown through water conversion in Fig. S3a, with oxidation of iron in slag (Fig. S3b). The aggregate non-metallic slag produced the most H<sub>2</sub>, yielding 1.01 mmol-H<sub>2</sub> g<sup>-1</sup>, followed by quenched slag with 0.76 mmol-H<sub>2</sub> g<sup>-1</sup>. Slag fines and aged fines produced less H<sub>2</sub>, with 0.34 and 0.07 mmol-H<sub>2</sub> g<sup>-1</sup>, respectively.

The varying amounts of H<sub>2</sub> produced from different BOF slags highlight the important role of slag handling. Quenched slag, removed from the BOF and cooled as approximately 0.15 m chunks, and aggregate non-metallic slag, separated into chunks larger than 3/8", have small surface areas, limiting oxidation of reduced iron during cooling and storage and thus giving high H<sub>2</sub> production.

## ***Technoeconomic Analysis Methods***

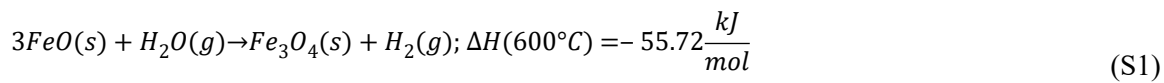
For the technoeconomic analysis, four major cases were considered. Point-source Na<sub>2</sub>CO<sub>3</sub> looping, point-source baseline, air CO<sub>2</sub> Na<sub>2</sub>CO<sub>3</sub> looping, and air CO<sub>2</sub> baseline. Due to the complexity of the system, the process design is first outlined in the following sections for point-source looping, followed by additional sections highlighting the adjustments made for the other cases. The assumptions from the first case hold true unless stated otherwise.

### *TEA – Point-Source Looping*

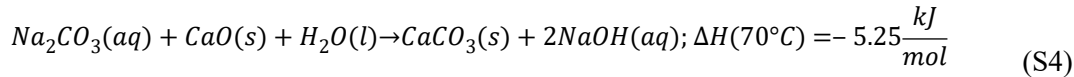
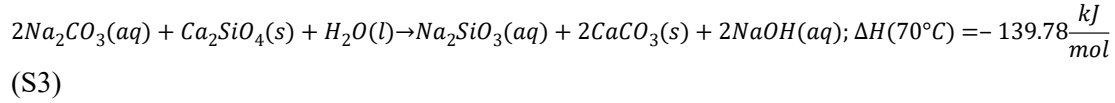
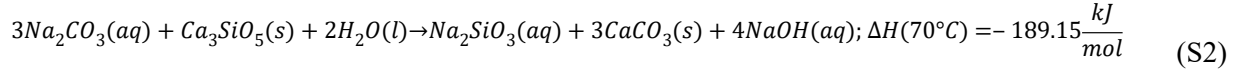
#### *Process Chemistry and Thermodynamics*

In the blast furnace-BOF steel making process, iron ore (Fe<sup>3+</sup>) is reduced to iron in the blast furnace and then transferred to the BOF where O<sub>2</sub> is impinged at high pressure to further remove carbon. During the BOF process, fluxes are added to the steel to remove additional impurities. The major flux, CaO, reacts with SiO<sub>2</sub> to form various types of calcium silicates, mainly Ca<sub>2</sub>SiO<sub>4</sub> and Ca<sub>3</sub>SiO<sub>5</sub>, which float to the top of the melt in the BOF furnace where they can be separated from the steel. Some iron (Fe<sup>2+</sup>) from the steel is separated along with the calcium silicates due to incomplete reduction from the blast furnace or oxidation during the BOF process. After the steel slag is separated, the process studied in this paper begins.

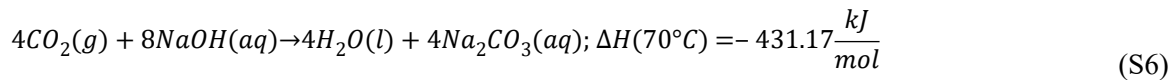
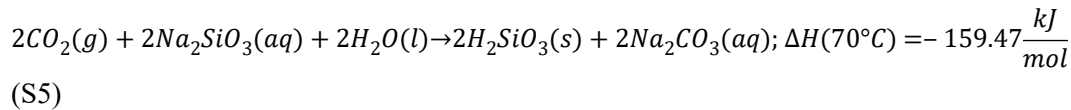
The process begins with H<sub>2</sub> production by reacting steam with the steel slag at 600°C (Step 1). As outlined in Eqn S1, water vapor reacts with part of Fe<sup>2+</sup> to form H<sub>2</sub> and Fe<sup>3+</sup>. The exothermic reaction can be directly carried out by flowing water over high temperature slag which uses remaining heat from the BOF furnace to form high temperature steam. The oxidized iron remains an unreactive component through the remaining process, making the first step optional. As a simplified reaction equation neglecting other cations mixed with Fe ions in slag, we can write



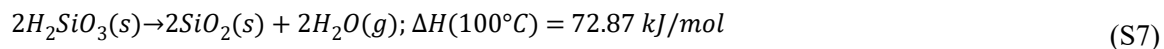
The steel slag can then be cooled and milled into a powder which is fed into the cyclic carbonation and CO<sub>2</sub> capture steps. The carbonation step (Step 2) considers an aqueous solution of Na<sub>2</sub>CO<sub>3</sub> reacting with Ca<sub>3</sub>SiO<sub>5</sub>, Ca<sub>2</sub>SiO<sub>4</sub>, and CaO at mild temperatures such as room temperature and 70°C, as shown in Eqns S2-4.



The CaCO<sub>3</sub> and other components in the carbonate-rich product can be filtered and removed from the solution. The remaining basic solution can then react with CO<sub>2</sub> in a flue gas or in air. Both the Na<sub>2</sub>SiO<sub>3</sub> and NaOH can capture CO<sub>2</sub> at low temperatures to regenerate Na<sub>2</sub>CO<sub>3</sub> (Eqns S5 and S6). It is important to note that the reaction enthalpy of CO<sub>2</sub> with NaOH is quite high which will result in low grade waste heat that will need to be managed. In addition, a portion of the water consumed in Eqns S2-4 will be regenerated in Eqn S6.



The final step is to filter the H<sub>2</sub>SiO<sub>3</sub> from the solution and dry it to form amorphous SiO<sub>2</sub> (Eqn S7), so that the remaining water consumed in Eqns S2-4 is regenerated. The amorphous SiO<sub>2</sub> can then be washed with water and sold. From this point, additional steel slag can be added to the Na<sub>2</sub>CO<sub>3</sub> solution, and the cycle can continue.



The reaction enthalpies were determined using the View Data function in FactSage 8.3, which provided enthalpy values for individual phases.<sup>16,17</sup> Solution enthalpy values not found in FactSage - Na<sub>2</sub>CO<sub>3</sub>, Na<sub>2</sub>SiO<sub>3</sub>, NaOH, and Ca(OH)<sub>2</sub> – are referenced from NIST<sup>18</sup>. Both data sources use the same standard reference state of 298 K and 1 bar for enthalpy values, ensuring consistency when combining FactSage and NIST thermochemical data.

### *Mass and Energy balance*

To quantify the molar content of active phases in steel slag during the reactions, a combination of XRD refinement and TGA was employed. First, Rietveld refinement of XRD data was performed to determine the fraction of crystalline phases present in the slag (Table S3). Ca<sub>3</sub>SiO<sub>5</sub>, Ca<sub>2</sub>SiO<sub>4</sub>, and CaO are considered active components in the carbonation reaction. Mg<sub>0.8</sub>Fe<sub>0.2</sub>O is reactive in H<sub>2</sub> production and Ca<sub>2</sub>Fe<sub>2</sub>O<sub>5</sub> is unreactive. Since amorphous phases cannot be directly quantified through XRD, their contribution was indirectly accounted for using TGA. The total amount of CO<sub>2</sub>

mineralized during carbonation was determined by measuring the mass loss associated with  $\text{CaCO}_3$  decomposition in TGA – 2.79 mmol  $\text{CO}_2$  per gram of slag. The  $\text{CO}_2$  mineralized was determined for the carbonation of quenched slag at 45°C with 4%  $\text{CO}_2$  (Figs. 2a and S5a). By correlating our experimental  $\text{CO}_2$  uptake with relative fractions of calcium-containing phases via Eqns S2-6, the absolute fractions of reacted  $\text{Ca}_3\text{SiO}_5$ ,  $\text{Ca}_2\text{SiO}_4$ , and  $\text{CaO}$  were estimated. These fractions were then normalized to 1 g to obtain the molar quantities of each reacted phase in 1 g slag (Table S4).

The mass balance was initiated with the calculated amounts of  $\text{Ca}_3\text{SiO}_5$ ,  $\text{Ca}_2\text{SiO}_4$ , and  $\text{CaO}$ . The  $\text{Na}_2\text{CO}_3$  and water amounts were directly scaled from experiments with mass ratios of 2.5:1  $\text{Na}_2\text{CO}_3$  to slag and 50:1 water to slag. From there, the amount of  $\text{FeO}$  in the steel slag was assumed based on experimental  $\text{H}_2$  production of 16.99 std. mL  $\text{H}_2/\text{g}$  slag. Then 100,000 tons of  $\text{CO}_2$  captured annually was input into the system. A wash ratio (mass of water to mass of solid) of 1.5 was used to calculate the amount of water required to wash the amorphous  $\text{SiO}_2$ . The mass change of water after washing the  $\text{SiO}_2$  was assumed to be negligible. Using these inputs the mass balance was completed and reduced to mass per hour (Table S5). The mass in and out of the system are highlighted in Fig. 3a along with the process diagram.

Heat balance in the reactors was calculated by considering the heat loss from natural convection from the reactor and heat generation or consumption due to exo/endergonic reaction. The cycle time was assumed to be 0.5 h based on the experimental procedure. Using the mass flow rate of materials, the reactors were sized based on volume, and the reactors were assumed to be a cube to estimate surface area interfacing with the environment. The density of steel slag and carbonated steel slag (carbonate-rich product), were assumed to be 3000  $\text{kg}/\text{m}^3$  and 3350  $\text{kg}/\text{m}^3$  respectively.<sup>19,20</sup> The density of silicic acid was assumed to be close to that of silica gel 600  $\text{kg}/\text{m}^3$ .<sup>21</sup> The density of the solution phase was calculated from Hitchcock and McIlhenny<sup>22</sup>, and the effect of  $\text{Na}_2\text{CO}_3$  and  $\text{NaOH}$  on density of solution were considered. Once the surface area was calculated, the heat loss to environment could be estimated using an assumed overall heat transfer coefficient of 0.003  $\text{kW}/(\text{m}^2\text{K})$  which was related to an insulated reactor into still air.<sup>23</sup> The heat generated or consumed during the reaction was calculated using the reaction enthalpy and mols of feedstock in the reactor. The active cooling of a reactor via cooling water or active heating of a reactor was then calculated by considering both the heat loss via reactor wall and the reaction heats.

Heat transfer for materials between reactors was calculated using literature enthalpy data or specific heat data. The specific heat of steel slag was assumed to be 935  $\text{J}/\text{kgK}$ .<sup>24</sup> Steel slag exiting the BOF at 1650°C is allowed to naturally cool to 653°C. At 653°C, the heat available is enough to generate steam from the flow of water into Step 1. The steam reacted slag leaving Step 1 must then be cooled down to 70°C which is required for Step 2 and 3. The temperature for Step 2 and 3 was increased from 45°C in our experiments to 70°C to prevent a small temperature difference in the heat exchanger to dissipate the reaction heat, which would otherwise require a larger surface area and increase costs. At 70°C, performance is expected to be similar, or better than, the experimental results at 45°C. The heat from the steel slag between Steps 1 and 2 can then be used to power a steam power cycle and dry the silicic acid in Step 4. Milling and filtering are assumed to happen at 70°C. After the second filtering process, the silicic acid must be heated from 70°C to 100°C and then the water vapor that forms must be cooled to 70°C for return to Step 2. The specific

heat of silicic acid was calculated from FactSage as 1050 J/kgK.<sup>16,17</sup> Additionally, the flue gas (point-source CO<sub>2</sub>) was assumed to enter the system at 83°C coming from a natural gas combined cycle power plant.<sup>25</sup> The flue gas releases heat to the Step 3 reaction and was assumed to have a specific heat of 1050 J/kgK.<sup>26</sup>

The heat transfer components are highlighted in Fig. 3a. The H<sub>2</sub> production reactor does not involve active heat dissipation or supply because the heat loss to the environment was about equal to exothermic heat generation by altering the reaction time and reactor volume for H<sub>2</sub> production. The waste heat from the steel slag on the conveyor is used to dry the silicic acid while releasing the remaining heat to the atmosphere. The heat exchanger on the carbonation reactor handles the exothermic reaction heat and heat release from the condensation of water vapor from the dryer. The analysis is for steady state operation and thus initial heating of water and Na<sub>2</sub>CO<sub>3</sub> feedstock are ignored. The heat exchanger on the CO<sub>2</sub> capture spray tower also handles exothermic reaction heat as well as sensible heat from the flue gas.

Electric energy input for the process was calculated for the conveyor belt (between Step 1 and milling), milling, filtering, stirring, pumping solution (between Step 2 and 3), and fan-driven gas flow which were determined to be the major energy consumption processes. Energy input for transporting water vapor from Step 4 to 2 was determined to be negligible. The power requirement of the conveyor belt was 0.72 kW/Mg/h per km of horizontal distance.<sup>23</sup> Milling steel slag was assumed to consume 3.84 kWh/ton<sup>27</sup> and filtering consumes 0.18 kWh/m<sup>3</sup>-water.<sup>28</sup> Agitation is required for Step 2 and washing SiO<sub>2</sub> and the energy consumption was assumed to be 0.1 kW/m<sup>3</sup>.<sup>23</sup> The energy requirement for the pumps and fans are calculated based on assumptions from Carbon Engineering<sup>29</sup> and are detailed in the *Discussion of Specific Equipment* section. The power requirements for the individual components are shown in Fig. 3a.

Four energy scenarios for providing electricity were considered for each case: 1) Energy purchased from an external solar grid, 2) Internal solar photovoltaic (PV) system with integrated 16-hour battery storage, 3) Internal wind turbines with integrated 16-hour battery storage, and 4) Internal steam power plant powered by waste heat from the steel slag. Energy purchased from an external solar grid was assumed to be \$0.0576/kWh.<sup>30</sup> The internal solar PV system was designed to be in Cincinnati, Ohio (4.5 sun hours) with an inefficiency factor of 1.2. The solar panel cost was assumed as \$1.1/W.<sup>31</sup> To account for intermittency of solar energy, a grid scale battery system was sized for 16 hours of electricity with a cost of \$92/kWh.<sup>32</sup> The internal wind turbines were assumed to have an average installed cost of \$1370/kWh with a capacity factor of 36%.<sup>8</sup> Similarly to solar PV, a 16-hour battery system was included to accommodate the intermittency of wind energy. The steam power plant was designed as a real steam Rankine cycle with isentropic pump and turbine efficiencies of 0.8 and 0.9, respectively.<sup>33,34</sup> The state values are shown in Table S6. The steam power plant is powered by direct contact heat exchange from the steel slag to water as the working fluid directly after leaving the H<sub>2</sub> production reactor.

### *Capital Cost*

Capital cost of the system was estimated using data from engineering design textbooks.<sup>23,35</sup> To estimate the capital cost, the purchase cost, or free on-board cost (FOB cost), was calculated and additional factors were applied. The general equation for capital cost of equipment is shown as Eqn (S8).

$$Cost = \left[ (FOB\ cost)_{ref} \left( \frac{size}{size_{ref}} \right)^n \frac{CEPCI}{1000} (F_m f_{i,alloy}) \right] [F_i] \left[ \frac{(1 + F_o)}{F_u} \right]$$

(S8)

Where the FOB cost of reference equipment is multiplied by a ratio of sizes which corrects for economy of scale by the factor of n. If the size of the designed equipment was outside the range specified for n, then linear scaling was assumed to be conservative. The CEPCI is the Chemical Engineering Plant Cost Index where the CEPCI index is 1000 while the analysis considers the plant being manufactured in 2030 when the CEPCI index will be an assumed 725.  $F_m$  is the materials factor to account for purchasing equipment that is designed with materials other than carbon steel. The installation factor,  $F_i$ , considers installation costs such as electrical, piping, insulation, painting, concrete, and labor.  $F_i$  is independent of construction material for equipment and needs to be lowered by the factor  $f_{i,alloy}$ .  $F_o$  is the offsite investment factor which accounts for improvements to the site infrastructure and is assumed to be 0.4 for a new site.<sup>35</sup>  $F_u$  is the plant utilization factor and is assumed to be 0.95 as the plant can operate continuously. In the following sections, the equipment cost without  $F_i$ ,  $F_o$  and  $F_u$  is considered the FOB cost while the installed cost includes  $F_i$  and not  $F_o$  and  $F_u$ . The lifespan of the plant was assumed to be 50 years, and the lifespan of equipment was estimated (Table S7) to help determine their replacement schedule. The offsite factor,  $F_o$ , is not included in the price of the replacement equipment because additional improvements to the infrastructure are not needed. The FOB cost, installed costs, and total cost over 50 years for the equipment are detailed in Table S9 for electricity cases 1-3.<sup>23,35</sup> When a steam power plant is considered, the cost components for the power cycle are added and the size of the heat exchanger, cooling tower, and conveyor belt are updated (Table S10).

Additional capital costs include  $Na_2CO_3$ , water, and land. The initial feedstock of  $Na_2CO_3$  is based on a market price of \$1,042/ton.<sup>36</sup> Water is required for Step 2 and 3 reactions as well as the cooling tower. The initial water volume required to fill the cooling tower system consists of the water needed to fill the cooling tower basin and connected piping. A reasonable approximation is to assume that this volume is approximately twice the system's circulating flow rate. Water cost is set as \$1.58/ton.<sup>37</sup> The cost of land was estimated as 1% of the installed cost of equipment.<sup>23</sup> Additional land cost was included for the solar PV and wind turbine systems requiring 8.3 acres/MW and 85.25 acres/MW respectively.<sup>38,39</sup> The cost of land was assumed to be \$3,343/acre.<sup>40</sup>

### *Discussion of Specific Equipment*

**Carbonation Reactor:** Due to the high water-to-slag ratio, a large volume of solution is present in the carbonation reactor at any given time. To reduce costs, a concrete basin was sized for the carbonation reaction instead of a metal reactor. It is assumed that if the basin is open to air, any  $CO_2$  uptake from the atmosphere would form silicic acid during carbonation which would be negligible compared to the 4%  $CO_2$  during the capture step. This assumption does not affect the overall process and may even provide additional  $CO_2$  capture from the air. For mixing, top-entry propellers were sized for the open basin, assuming an agitation power requirement of 0.1 kW/m<sup>3</sup>.

**Gas Contactor System:** The design of the gas contactor system follows Carbon Engineering's air-contactor concept.<sup>29</sup> It includes a slab contactor equipped with packing for contacting the flue gas with the absorption solution, along with fans for gas handling and pumps for solution circulation. The capital cost is based on the required contactor frontal area, A, determined from Eqn (S9). The

reacted CO<sub>2</sub> mass flow rate,  $\dot{m}_{CO_2}$ , was assumed to correspond to 100,000 tons of CO<sub>2</sub> captured per year. The gas velocity,  $V$ , and density,  $\rho$ , were taken as 1.6 m/s and 0.92 kg/m<sup>3</sup>, respectively, representing the properties of the flue gas.<sup>41</sup> The CO<sub>2</sub> mass fraction,  $w_{CO_2}$ , was calculated from a 4% CO<sub>2</sub> concentration in air (corresponding to 6% by mass), and the capture fraction,  $X_{CO_2}$ , was set to the experimental value of 59%.

$$A = \frac{\dot{m}_{CO_2}}{V\rho w_{CO_2} X_{CO_2}} \quad (S9)$$

The total capital cost of the contactor was determined using Eqn (S10), where  $C_A$  is the capital cost per unit frontal area, valued at \$3700/m<sup>2</sup>,  $C_{pack}$  is the cost of the packing and fluid distributor, taken as \$250/m<sup>3</sup>, and  $D$  is the packing depth of 8.6 m.

$$C_{capital} = (C_A + C_{pack}D) * A * F_u \quad (S10)$$

The cost estimates reported in Carbon Engineering's study were originally based on 2008–2009 Alberta prices. To update these costs, conversion from Canadian dollars to U.S. dollars and adjustment to 2030 values were required. An exchange rate of 1.07 Canadian dollars per U.S. dollar was applied for 2008, and a CEPCI value of 575.4 was used for that year. It was also noted that Alberta capital costs during this period were approximately 30–50% higher than those on the U.S. Gulf Coast. To remain conservative in this analysis, the capital costs were therefore reduced by 40% to better represent projected U.S. conditions.

The fan pressure drop,  $\Delta P$ , and energy requirement,  $E$ , were calculated using Eqn (S11) and (S12). The fan efficiency,  $\eta_{fan}$ , was assumed to be 71%, but reduced by 15% (to 56%) to account for additional pump energy.

$$\Delta P = D7.4V^{1.4} \quad (S11)$$

$$E = \Delta PV / \eta_{fan} \quad (S12)$$

Mill: Since the installation cost was already incorporated into the FOB cost, an additional installation factor was omitted.<sup>23</sup>

Filters: The filtration rate was assumed to be 3 L/s/m<sup>2</sup>.<sup>23</sup> The selected rotary disk filters did not include a vacuum pump, so a rotary vane vacuum pump was sized separately for a single filter. Since the two filters are of similar size, the calculated pump cost was then multiplied by two to account for both units.

Dryer: The drying rate was assumed to be 0.27 g<sub>water</sub>/s/m<sup>2</sup> and the capacity was 35 kg/m<sup>2</sup>.<sup>23</sup>

Heat exchanger and cooling tower: The overall heat transfer coefficient for the heat exchanger was chosen as 1500 W/m<sup>2</sup>/°C for water to water.<sup>35</sup> For cooling reactors, the hot side (reactor) was designed to not change temperature. The minimum achievable temperature by the water was calculated by adding the wet bulb temperature, 23.8°C, to the approach temperature, 5.5°C, which results in 29.3°C.<sup>23</sup> The cooling capacity of the tower was chosen to be 8.3°C which leads to 29.3°C cold fluid out and 37.6°C cold fluid in.<sup>23</sup>

Belt Conveyor: The conveyor was designed to cool slag to the carbonation temperature after H<sub>2</sub> production. The radiative heat from the slag is used to dry the silicic acid. The conveyor belt was designed to have a width of 72 in (1.83 m) and a velocity of 3 m/s.<sup>42,43</sup> The slag was assumed to be a flat plate on the conveyor with a constant rate of cooling. Radiation and convection cooling were considered in the design with ambient conditions considered as air at 25°C. The radiation component was calculated using a steel slag emissivity of 0.81.<sup>44</sup> The convection component was calculated by using the Nusselt correlation for turbulent flow over a flat plate with constant heat flux conditions (Eqn S13).<sup>45</sup> Heat transfer was calculated using the average temperature formula provided in Eqn S14.<sup>46</sup> To determine the Reynolds number and convective heat transfer coefficients, an initial conveyor length of 100 m was assumed and later iteratively updated to match the calculated length. The total conveyor length was determined based on two sequential cooling stages: (1) from the outlet temperature of the H<sub>2</sub> production step to the slag outlet temperature from the steam power plant, and (2) from that steam power plant outlet temperature to the carbonation temperature. For energy scenarios 1–3 (no steam power cycle included), the total conveyor length includes both cooling stages. For the steam power plant scenario, only the second cooling stage was considered.

$$Nu_x = 0.0308Re_x^{4/5}Pr^{1/3} \quad (S13)$$

$$T_{avg} = \frac{T_{in}^5 - T_{out}^5}{5(T_{in} - T_{out})} \quad (S14)$$

Steam Power Cycle: The steam power cycle was designed with a single-valve, single-stage steam turbine, a centrifugal pump, a direct-contact barometric condenser, and a direct-contact heat exchanger for steam generation. The turbine operates at 20 bar with 100°C superheat, which adds a 0.97 factor to the FOB cost. Steam generation assumes direct contact between the hot steel slag and the working fluid, requiring a vertical pressure vessel as a direct-contact heat exchanger. To size this vessel, the volume of steel slag and steam within the system at any given time was determined. The convective heat transfer coefficient was estimated using the Wakao and Kaguei Nusselt correlation for heat transfer in a packed bed (Eqn S15).<sup>47</sup> The Nusselt number was calculated based on an assumed heat transfer time of 10 minutes, a slag particle diameter of 0.05 m, and a reactor diameter of 1 m. Once the convection coefficient was determined, the actual heat transfer time was calculated. The total slag surface area available for heat transfer was assumed to be the calculated conveyor belt surface area. The final calculated heat transfer time was found to be within the same order of magnitude as the initial assumption. An additional cost factor of 1.15 was included for the pressure vessel to handle 2 MPa.

$$Nu_x = 2 + 1.1Pr^{1/3}Re^{0.6} \quad (S15)$$

After the steel slag leaves the direct-contact heat exchanger, it is at 245°C before entering the belt conveyor. The heat exchanger and cooling tower were increased in size to handle the heat release from the condenser in the steam power cycle, if included.

#### *Annualized Capital Cost*

The capital cost of the plant was calculated using the annualized capital cost formula shown in Eqn S16, where the total capital cost is multiplied by the capital recovery factor which depends on

interest rate,  $i$ , and lifespan of the plant,  $n$ . The interest rate was assumed to be 5%<sup>48</sup> and the lifespan of the plant was estimated at 50 years.

$$\text{Annualized Capital Cost} = \text{Total Capital Cost} * \left( \frac{i(1+i)^n}{(1+i)^n - 1} \right) \quad (\text{S16})$$

### *Operating Costs*

The operating costs include maintenance, labor,  $\text{Na}_2\text{CO}_3$  replenishment, and water inlet for  $\text{H}_2$  production and washing  $\text{SiO}_2$ . Maintenance of equipment was assumed to be 4% of the total installed cost of the equipment annually. Maintenance for solar PV and wind turbines were assumed to be \$22/kW/year and \$39/kW/year, respectively.<sup>30,49</sup> Maintenance for grid scale batteries was assumed to be 2.5% of the capital cost.<sup>50</sup> An operating and maintenance cost equal to 5% of the total capital cost was included for the gas contactor system.<sup>29</sup> For the case of using external solar grid electricity, the plant is operated by 2 laborers per shift. An additional laborer is added per shift for the other cases where electricity is generated on site. The laborers are paid an average wage of \$38.50/hour.<sup>51</sup>  $\text{Na}_2\text{CO}_3$  is estimated to be replenished 2 times a year for the market price of \$1,042/ton. Water cost for  $\text{H}_2$  production and washing  $\text{SiO}_2$  is considered \$1.58/ton. Evaporation is considered negligible, and the water is assumed to not need replenishment for Step 2 and 3 or the cooling tower.

### *Levelized Cost of Electricity*

The levelized cost of electricity (LCOE) was calculated by dividing the sum of the annualized capital cost and operating cost by the total annual electricity generation (Eqn S17).

$$\text{LCOE} = \frac{\text{Annualized Capital Cost} + \text{Annual Operating Cost}}{\text{Annual Electricity Generation (MWh}_e\text{)}} \quad (\text{S17})$$

### *Revenues*

Revenues from  $\text{H}_2$ , carbonate-rich product, precipitated silica, and the 45Q tax credit were accounted for. The  $\text{H}_2$  selling price was assumed to be \$2/kg.<sup>52</sup> The selling price of the point-source  $\text{Na}_2\text{CO}_3$  looping carbonate-rich product was assumed to be \$26/ton.<sup>53</sup> Precipitated silica has a selling price ranging from \$600 to \$1200 per ton, depending on purity.<sup>54</sup> The price was set at \$600 to be conservative. Finally, the 45Q tax credit provides \$85/ton of  $\text{CO}_2$  captured for projects that convert point-source  $\text{CO}_2$  into useful products.<sup>55</sup>

### *Breakeven Time*

The breakeven time was calculated by dividing the total capital expenses by yearly profit. The profit is the difference between yearly revenue and yearly operating expenses (Eqn (S18)).

$$\text{Breakeven Time (years)} = \frac{\text{CAPEX}}{\text{Yearly Revenue} - \text{Yearly OPEX}} \quad (\text{S18})$$

The breakeven time was calculated for the scenario where electricity is provided from an external solar grid and is shown:

$$CAPEX = Equipment + Land + Water + Na_2CO_3 = \$39,144,316 + \$142,708 + \$14,437 + \$242,124 = \$39,543,585$$

Revenue

$$\begin{aligned} &= H_2 + Carbonated\ Slag + Silica + 45Q\ Tax\ Credit = \left(\frac{\$2}{kg_{H_2}}\right)\left(1,244,677\frac{kg_{H_2}}{year}\right) + \left(\frac{\$26}{ton_{carbonate}}\right)\left(1,244,677\frac{kg_{H_2}}{year}\right) \\ &+ \left(\frac{\$600}{ton_{silica}}\right)\left(37,599\frac{ton_{silica}}{year}\right) + \left(\frac{\$85}{ton_{CO_2}}\right)\left(100,000\frac{ton_{CO_2}}{year}\right) = \$56,602,824 \end{aligned}$$

OPEX

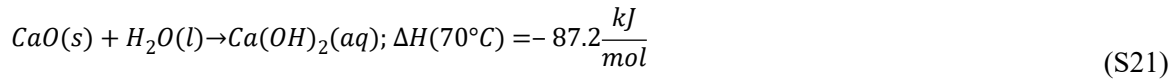
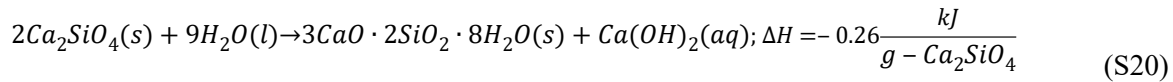
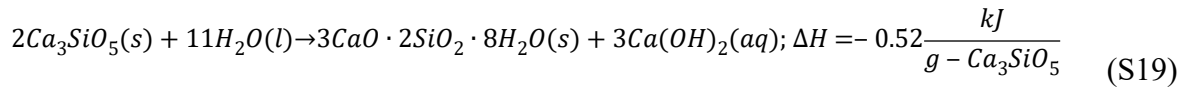
$$\begin{aligned} &= Maintenance + Labor + Water + Na_2CO_3 + Electricity = \$564,980 + \$674,520 + \$62,280 \\ &= \$3,000,202 \end{aligned}$$

$$Breakeven\ Time = \frac{\$39,543,585}{\frac{\$56,602,573}{year} - \frac{\$3,000,202}{year}} = 0.8\ years$$

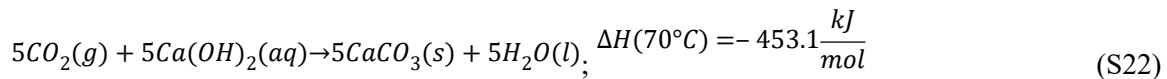
### TEA – Point-Source Baseline

#### *Process Chemistry and Thermodynamics*

The H<sub>2</sub> production step in the baseline case follows the same reaction as the looping scenario. After H<sub>2</sub> production, the steel slag is cooled and milled into a powder which is fed into cyclic hydration and CO<sub>2</sub> capture steps. The hydration step (Step 2) considers water reacting with Ca<sub>3</sub>SiO<sub>5</sub>, Ca<sub>2</sub>SiO<sub>4</sub>, and CaO as shown in Eqns S19-21. The hydration of Ca<sub>3</sub>SiO<sub>5</sub>, Ca<sub>2</sub>SiO<sub>4</sub>, forms 3CaO•2SiO<sub>2</sub>•8H<sub>2</sub>O referred to as calcium silicate hydrate (CSH). The heat of hydration and reaction equations for Ca<sub>3</sub>SiO<sub>5</sub> and Ca<sub>2</sub>SiO<sub>4</sub> are referenced from Mindess et al.<sup>56</sup>



The CSH and other components in the hydrated steel slag can be filtered and removed from the solution. The remaining Ca(OH)<sub>2</sub> solution can then react with CO<sub>2</sub> in a flue gas or in air at low temperatures to precipitate CaCO<sub>3</sub>. Only a portion of the water consumed in Eqns S19-21 will be regenerated in Eqn S22 which leads to an overall deficit of water in the cycle which requires replenishment.



The CaCO<sub>3</sub> can then be filtered from the water. From this point, additional steel slag and makeup water can be added, and the cycle can continue.

#### *Mass and Energy balance*

The molar content of actively reacted phases was quantified in the same way as the point-source looping but using the hydration reaction equations and our experimentally measured 0.34 mmol CO<sub>2</sub> mineralized per gram of slag. The CO<sub>2</sub> mineralized was determined for the baseline carbonation of quenched slag at 45°C with 4% CO<sub>2</sub> (Fig. 2a and S5b). The molar quantities of each phase in the slag are shown in Table S4.

The major differences between the looping and baseline scenario in mass balance include: (1) the baseline produces hydrated slag instead of carbonated slag (carbonate-rich product) in Step 2, (2) the baseline produces precipitated CaCO<sub>3</sub> during the CO<sub>2</sub> capture step instead of silicic acid, (3) the process consumes water in the baseline which requires makeup. For direct comparison to the looping scenario the baseline considers the outlet of hydrated slag plus precipitated CaCO<sub>3</sub> as the supplementary cementitious material product (carbonate-rich product). The mass balance for the point-source baseline is shown in Table S5 and Fig. S7a.

Active heating or cooling needed for the reactors was once again calculated by considering the heat loss from natural convection and heat generation or consumption due to exo/endermic reactions. To calculate the reactor size, the density of hydrated steel slag was input as 2604 kg/m<sup>3</sup>.<sup>57</sup> It was assumed that Ca(OH)<sub>2</sub> concentration has no effect on solution density, as a saturated solution would have a density close to that of water.<sup>58</sup> The density of CaCO<sub>3</sub> was assumed to be 2700 kg/m<sup>3</sup>.<sup>59</sup>

The heat transfer between the reactors was handled the same as looping scenario; however, there is no H<sub>2</sub>SiO<sub>3</sub> production and therefore no drying step is necessary. The heat from the steel slag on the conveyor belt is completely released to the atmosphere or partially used for driving steam power cycle. After the steam power plant, the steel slag leaves at 146°C. In addition, the makeup water is assumed to enter the hydration reactor at 25°C which requires heating to the reaction temperature of 70°C. The heating need is less than the exothermic heat release for Step 2. The heat balance is shown in Fig. S7a.

### *Capital Cost*

The process cost was estimated in the same manner as the looping scenario. For the point-source baseline, a CO<sub>2</sub> conversion of 7% was determined from the CO<sub>2</sub> capture step of baseline quenched slag at 45°C with 4% CO<sub>2</sub> in our experiments (Fig. 2a). The FOB cost, installed costs, and total cost over 50 years for the equipment are detailed in Table S11 for electricity cases 1-3. The updated steam power plant components are listed in Table S12. No Na<sub>2</sub>CO<sub>3</sub> is required for the process so there is no capital cost of Na<sub>2</sub>CO<sub>3</sub> included.

### *Operating Costs and Revenue*

The operating costs include maintenance, labor, and water inlet for H<sub>2</sub> production and makeup.

Revenues from H<sub>2</sub>, carbonate-rich product, and the 45Q tax credit were accounted for. The baseline considers the outlet of hydrated slag plus precipitated CaCO<sub>3</sub> as the carbonate-rich product. The selling price of the point-source baseline carbonate-rich product was assumed to be \$3.32/ton, which was scaled to have equal yearly revenue for carbonate-rich product as the point-source looping case, considering the mixed effects of larger product quantity and lower product carbonation extent of baseline product than looping.

### *TEA – Air CO<sub>2</sub> Looping*

The process chemistry and thermodynamics for the air CO<sub>2</sub> looping case is the same as the point-source looping. The molar content of actively reacted phases was quantified in the same way as the point-source looping, but with 0.83 mmol CO<sub>2</sub> mineralized per gram of slag. The CO<sub>2</sub> mineralized was determined for the carbonation of quenched slag at 24°C with air CO<sub>2</sub> by our experiment (Fig. 2c and S5c). The molar quantities of each phase in the slag are shown in Table S4.

The mass balance for the air CO<sub>2</sub> looping is shown in Table S5 and Fig. 4a.

The mass ratios of 1:1 Na<sub>2</sub>CO<sub>3</sub> to slag and 100:1 water to slag were directly adopted from our experiments. Additionally, the carbonation time was 15 minutes to be consistent with experiments. The CO<sub>2</sub> capture step is assumed to take 1.5 hours, with one batch of solution cycling in and out of the air contactor system every 15 minutes. The air was assumed to enter the system at 25°C. Due to the large mass of air entering the system, the exothermic heat release from the reaction of NaOH/Na<sub>2</sub>SiO<sub>3</sub> solution with CO<sub>2</sub> can be removed with a negligible air temperature rise. Additionally, during the carbonation step, the increase in temperature of the solution from exothermic reaction heat is negligible due to the large water to slag ratio. This allows the heat exchanger and cooling tower for the carbonation and air contactor system to be removed. The heat balance is shown in Fig. 4a.

Due to the large amount of electricity needed for the secondary processes (conveying, milling, filtering, stirring, pumping, and fan-driven gas flow), the steel slag input temperature needed to be increased for an internal steam power plant to supply electricity. Therefore, steel slag enters the system at 1067°C which supplies enough power to heat water to 1000°C where H<sub>2</sub> production occurs. After the steam power plant, the steel slag leaves at 176°C which still supplies enough heat to dry the H<sub>2</sub>SiO<sub>3</sub>.

The process cost was estimated in the same manner as the previous cases. For the air CO<sub>2</sub> looping a CO<sub>2</sub> conversion of 35% was determined from the CO<sub>2</sub> capture step of quenched slag at 24°C in our experiment (Fig. 2c). For the air contactor design, an air density of 1.24 kg/m<sup>3</sup> was assumed, along with a CO<sub>2</sub> mass fraction of 0.06% corresponding to an atmospheric concentration of 400 ppm. The FOB cost, installed costs, and total cost over 50 years for the equipment are detailed in Table S13 for electricity supply methods 1-3. The updated steam power plant components are listed in Table S14.

Revenues from H<sub>2</sub>, carbonate-rich product, precipitated silica, and the 45Q tax credit were accounted for. The selling price of the air CO<sub>2</sub> looping carbonate-rich product was assumed to be \$26/ton.<sup>53</sup> The 45Q tax credit provides \$180/ton of CO<sub>2</sub> captured for projects that convert air CO<sub>2</sub> into useful products.<sup>55</sup>

The breakeven time was calculated using Eqn S18 for the scenario where electricity is provided from an external solar grid and is shown:

$$CAPEX = Equipment + Land + Water + Na_2CO_3 = \$202,246,954 + \$782,764 + \$53,290 + \$325,554 = \$203,408,562$$

Revenue

$$= H_2 + Carbonated Slag + Silica + 45Q Tax Credit = \left( \frac{\$2}{kg_{H_2}} \right) \left( 4,183,915 \frac{kg_{H_2}}{year} \right) + \left( \frac{\$26}{ton_{carbonate}} \right) \left( 37,599 \frac{ton_{silica}}{year} \right) + \left( \frac{\$180}{ton_{CO_2}} \right) \left( 100,000 \frac{ton_{CO_2}}{year} \right) = \$122,590,794$$

OPEX

$$= Maintenance + Labor + Water + Na_2CO_3 + Electricity = \$3,898,964 + \$674,520 + \$81,500 = \$14,784,426$$

$$Breakeven Time = \frac{\$203,408,562}{\frac{\$122,590,794}{year} - \frac{\$14,784,426}{year}} = 1.9 \text{ years}$$

### TEA – Air CO<sub>2</sub> Baseline

The process chemistry and thermodynamics for the air CO<sub>2</sub> baseline case is the same as the point-source baseline. The molar content of active phases was quantified in the same way as the point-source baseline, but with 0.23 mmol CO<sub>2</sub> mineralized per gram of slag. The CO<sub>2</sub> mineralized was determined for the baseline carbonation of quenched slag at 24°C in our experiment (Fig. 2c). The molar quantities of each reacted phase in the slag are shown in Table S4.

The mass balance for the air CO<sub>2</sub> baseline is shown in Table S5 and Fig. S7b.

Similarly to the air CO<sub>2</sub> looping case, the CO<sub>2</sub> capture step takes place at 25°C due to the large amount of air entering the system and cooling the solution. The heat balance is shown in Fig. S7b.

Steel slag was assumed to enter the system at the same temperature as the air CO<sub>2</sub> looping scenario. Therefore, steel slag enters the system at 1067°C which supplies enough power to heat water to 1000°C where H<sub>2</sub> production occurs. Due to the high electricity demand, waste heat from the slag was insufficient to meet the process requirements. An additional 18.5 MW of grid electricity was supplied, resulting in the steel slag exiting the power cycle at 196°C.

The process cost was estimated in the same manner as the previous cases. For the air CO<sub>2</sub> baseline a CO<sub>2</sub> conversion of 9% was determined from the CO<sub>2</sub> capture step of baseline quenched slag at 24°C in our experiment (Fig. 2c). The FOB cost, installed costs, and total cost over 50 years for the equipment are detailed in Table S15 for electricity cases 1-3. The updated steam power plant components are listed in Table S16.

Revenues from H<sub>2</sub>, carbonate-rich product, and the 45Q tax credit were accounted for. The selling price of the air CO<sub>2</sub> baseline carbonate-rich product was assumed to be \$7.24/ton, which was scaled to have equal yearly revenue for carbonate-rich product as the air CO<sub>2</sub> looping case, considering the mixed effects of larger product quantity and lower product carbonation extent of baseline product than looping. The 45Q tax credit provides \$180/ton of CO<sub>2</sub> captured for projects that convert air CO<sub>2</sub> into useful products.

## References

- 1 A. O. Oni, K. Anaya, T. Giwa, G. Di Lullo and A. Kumar, *Energy Conversion and Management*, 2022, **254**, 115245.
- 2 P. Kadarno, D. S. Park, N. Mahardika, I. D. Irianto and A. Nugroho, *J. Phys.: Conf. Ser.*, 2019, **1198**, 042015.
- 3 M. S. Masaki, L. Zhang and X. Xia, in *2017 36th Chinese Control Conference (CCC)*, IEEE, Dalian, China, 2017, pp. 2767–2772.
- 4 CDW Engineering, Average Life Expectancies, <https://www.cdwengineering.com/average-life-expectancies/>, (accessed 24 March 2025).
- 5 A. H. Landfield and V. Karra, *Resources, Conservation and Recycling*, 2000, **28**, 207–217.
- 6 B. Nehme, N. K. M'Sirdi, T. Akiki, A. Naamane and B. Zeghondy, in *Predictive Modelling for Energy Management and Power Systems Engineering*, Elsevier, 2021, pp. 27–62.
- 7 P. Shao, K. Darcovich, T. McCracken, G. Ordorica-Garcia, M. Reith and S. O'Leary, *Chemical Engineering Journal*, 2015, **268**, 67–75.
- 8 R. Wisner, M. Bolinger, B. Hoen, D. Millstein, J. Rand, G. Barbose, N. Darghouth, W. Gorman, S. Jeong, E. O'Shaughnessy and B. Paulos, .

- 9 T. Capurso, L. Bergamini and M. Torresi, *Energy Conversion and Management*, 2022, **256**, 115341.
- 10 W. Cole and A. Frazier, *Cost Projections for Utility-Scale Battery Storage*, 2019.
- 11 J. Sorrels, A. Baynham, D. Randall and L. Randall, in *EPA Air Pollution Control Cost Manual*, 2021.
- 12 M. Ebrahimi and A. Keshavarz, in *Combined Cooling, Heating and Power*, Elsevier, 2015, pp. 35–91.
- 13 D. Singh, S. Mishra and R. Shankar, *Environ Sci Pollut Res*, 2023, **30**, 120010–120029.
- 14 D. Bharathan, E. Hoo and P. D’Errico, *An assessment of the use of direct contact condensers with wet cooling systems for utility steam power plants*, 1992.
- 15 P. Li, Y. Chen, X. Li, B. Yan, D. Chen and H. Guo, *International Journal of Hydrogen Energy*, 2020, **45**, 17140–17152.
- 16 C. W. Bale, E. Bélisle, P. Chartrand, S. A. Dechterov, G. Eriksson, K. Hack, I.-H. Jung, Y.-B. Kang, J. Melançon, A. D. Pelton, C. Robelin and S. Petersen, *Calphad*, 2009, **33**, 295–311.
- 17 C. W. Bale, P. Chartrand, S. A. Decterov, G. Eriksson, K. Hack, R. Ben Mahfoud, J. Melançon, A. D. Pelton and S. Petersen, *Calphad*, 2002, **26**, 189–228.
- 18 J. J. Reed, 2020.
- 19 M. Díaz-Piloneta, M. Terrados-Cristos, J. V. Álvarez-Cabal and E. Vergara-González, *Materials*, 2021, **14**, 3587.
- 20 J. Li, C. Wang, W. Ni, S. Zhu, S. Mao, F. Jiang, H. Zeng, X. Sun, B. Huang and M. Hitch, *Minerals*, 2022, **12**, 246.
- 21 T. Kawaguchi, H. Hishikura, J. Iura and Y. Kokubu, *Journal of Non-Crystalline Solids*, 1984, **63**, 61–69.
- 22 L. B. Hitchcock and J. S. McIlhenny, *Ind. Eng. Chem.*, 1935, **27**, 461–466.
- 23 D. R. Woods, *Rules of thumb in engineering practice*, John Wiley [distributor], Chichester, 2007.
- 24 J. Wang and Y. Huang, *Journal of Cleaner Production*, 2023, **395**, 136289.
- 25 S. Hughes, S. Leptinsky, M. Woods, A. Zoelle, N. Kuehn, T. Fout and G. Hackett, *Methodology for Estimating Performance and Cost of Natural Gas Combined Cycle Plants with Carbon Capture*, 2023.
- 26 L. Xu and J. Yuan, *Applied Thermal Engineering*, 2015, **90**, 366–375.
- 27 E. Mundy, 2024.
- 28 M. Grzegorzec, K. Wartalska and B. Kaźmierczak, *International Communications in Heat and Mass Transfer*, 2023, **143**, 106674.
- 29 G. Holmes and D. W. Keith, *Phil. Trans. R. Soc. A.*, 2012, **370**, 4380–4403.
- 30 Annual Technology Baseline - Utility Scale PV plus Battery, <https://public.tableau.com/views/2023OPEX/Dashboard1?:embed=y&:toolbar=no&Technology=All,Utility-Scale%20PV-Plus-Battery&:embed=y&:showVizHome=n&:bootstrapWhenNotified=y&:apiID=handler2>, (accessed 21 March 2025).
- 31 Utility-Scale Solar, 2024 Edition: Empirical Trends in Deployment, Technology, Cost, Performance, PPA Pricing, and Value in the United States | Energy Markets & Policy, <https://emp.lbl.gov/publications/utility-scale-solar-2024-edition>, (accessed 23 March 2025).
- 32 S. Deorah, N. Abhyankar, S. Arora, A. Gambhir and A. Phadke, Estimating the Cost of Grid-Scale Lithium-Ion Battery Storage in India, <https://emp.lbl.gov/publications/estimating-cost-grid-scale-lithium>, (accessed 30 March 2025).
- 33 X. Ping, F. Yang, H. Zhang, W. Zhang, G. Song and Y. Yang, *Sustainable Energy Technologies and Assessments*, 2020, **42**, 100898.
- 34 C. Zhang, J. Fu, J. Kang and W. Fu, *J Braz. Soc. Mech. Sci. Eng.*, 2018, **40**, 61.
- 35 G. P. Towler and R. K. Sinnott, *Chemical engineering design: principles, practice, and economics of plant and process design*, Butterworth-Heinemann, Boston, MA, 2nd ed., 2013.
- 36 Sodium Carbonate- Bulk 2500 Pound Pallet, <https://cqconcepts.com/product/sodium-carbonate-bulk-2450-pound-pallet/>, (accessed 23 March 2025).
- 37 Rates for Water Service | Northern Ohio Rural Water, <https://www.norw.org/rates-water-service>, (accessed 23 March 2025).

- 38 S. Ong, C. Campbell, P. Denholm, R. Margolis and G. Heath, *Land-Use Requirements for Solar Power Plants in the United States*, 2013.
- 39 P. Denholm, M. Hand, M. Jackson and S. Ong, *Land Use Requirements of Modern Wind Power Plants in the United States*, 2009.
- 40 N. Abashidze and L. O. Taylor, *Land Economics*, 2023, **99**, 327–342.
- 41 L. Xu and J. Yuan, *Applied Thermal Engineering*, 2015, **90**, 366–375.
- 42 Industrial Belt Conveyors & Powered Conveyor Belt Systems, <https://heinrichbrothers.com/product/conveyor-systems/belt-conveyors/>, (accessed 24 March 2025).
- 43 High Speed Conveyors | Conveying Solutions | Dorner, <https://www.dornerconveyors.com/solutions/high-speed-conveyors>, (accessed 24 March 2025).
- 44 B. V. Rangavittal, H. Köchner and B. Glaser, *steel research int.*, 2024, 2400277.
- 45 T. L. Bergman and A. S. Lavine, *Fundamentals of heat and mass transfer*, John Wiley & Sons, Hoboken, NJ, Eighth edition., 2017.
- 46 V. K. Budama, N. G. Johnson, I. Ermanoski and E. B. Stechel, *International Journal of Hydrogen Energy*, 2021, **46**, 1656–1670.
- 47 N. Wakao and S. Kaguei, *Heat and mass transfer in packed beds*, Gordon and Breach Science Publishers, New York, 1982.
- 48 M. Penev, A. Gilbert, N. Rustagi, J. Kee, M. Koleva and M. Chung, *Capital Structure for Techno-Economic Analysis of Hydrogen Projects*, 2024.
- 49 Annual Technology Baseline - Distributed Wind, [https://atb.nrel.gov/electricity/2024/distributed\\_wind](https://atb.nrel.gov/electricity/2024/distributed_wind), (accessed 21 March 2025).
- 50 Annual Technology Baseline - Commercial Battery Storage, [https://atb.nrel.gov/electricity/2024/commercial\\_battery\\_storage](https://atb.nrel.gov/electricity/2024/commercial_battery_storage), (accessed 21 March 2025).
- 51 T. Schmitt, S. Leptinsky, M. Turner, A. Zoelle, C. White, S. Hughes, S. Homsy, M. Woods, H. Hoffman, T. Shultz and R. James Iii, *Cost and Performance Baseline for Fossil Energy Plants Volume 1: Bituminous Coal and Natural Gas to Electricity*, 2022.
- 52 Hydrogen Production, <https://www.energy.gov/eere/fuelcells/hydrogen-production>, (accessed 25 March 2025).
- 53 Q. Song, M.-Z. Guo, M. Zhang and T.-C. Ling, *Journal of Cleaner Production*, 2024, **469**, 143214.
- 54 Intratec, Silicon Dioxide Prices | Historical and Current, <https://www.intratec.us/chemical-markets/silicon-dioxide-price>, (accessed 25 March 2025).
- 55 45Q Tax Credit for Carbon Capture Projects, <https://carboncapturecoalition.org/resource/45q-tax-credit-for-carbon-capture-projects/>, (accessed 12 November 2025).
- 56 S. Mindess, J. F. Young and D. Darwin, *Concrete*, Prentice Hall, Upper Saddle River, NJ, 2. ed., 2003.
- 57 A. J. Allen, J. J. Thomas and H. M. Jennings, *Nature Mater*, 2007, **6**, 311–316.
- 58 R. G. Bates, V. E. Bower and E. R. Smith, *J. RES. NATL. BUR. STAN.*, 1956, **56**, 305.
- 59 S. Teir, S. Eloneva and R. Zevenhoven, *Energy Conversion and Management*, 2005, **46**, 2954–2979.